Supporting Information

Wet climate and transportation routes accelerate spread of human plague

Contents

1. Locations and times of human plague occurrences in China during the third pandemic

Plague data were collected from multiple sources of historical records of plague incidence, investigation and identification of plague patients and graves and surveillances[S1]. The political centres of the counties (Fig. 1A, Supporting Information, Fig. S1) were plotted using the Krasovsky 1940 Albers projection in ArcGIS 9.2 (ESRI) (Fig. 1A and Supporting Information, Fig. S1).

Figure S1. Locations and times of human plague occurrences in China during the third pandemic. Map of human plague occurrences in China during the third pandemic. Colors of the points indicate the first year of recorded human plague in different counties. Names and locations of infected provinces are also shown. Note: only regions with confirmed plague cases are shown.

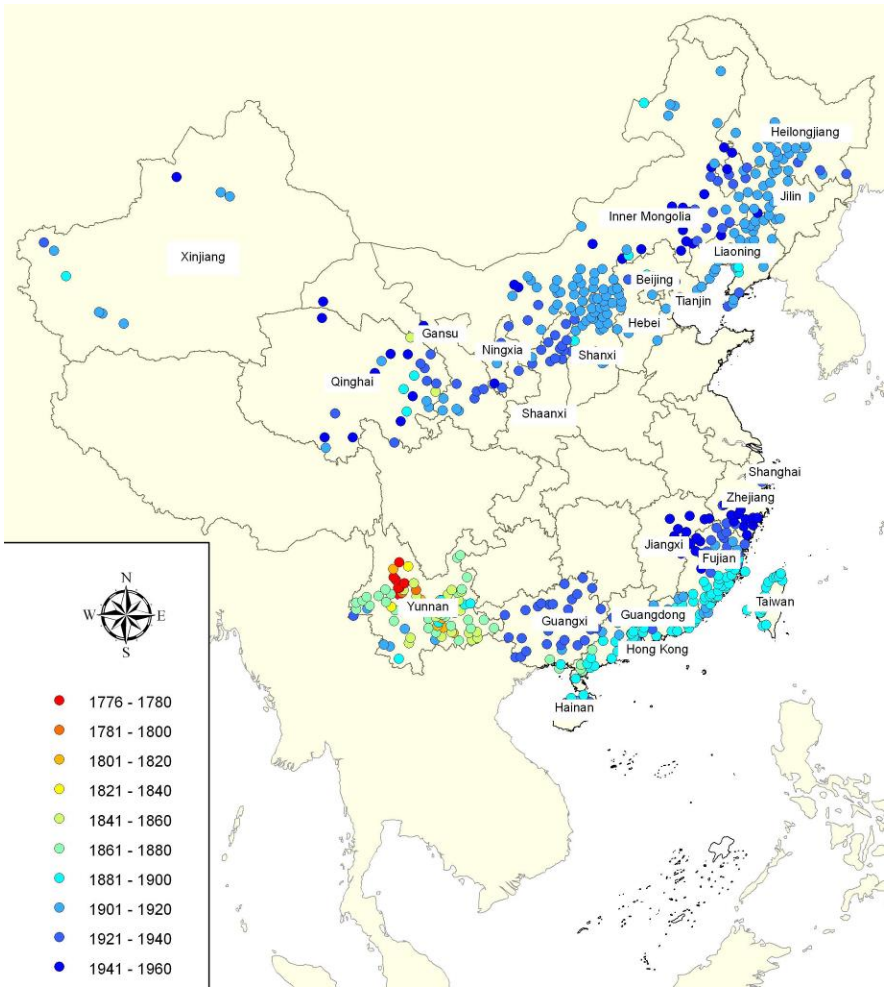

2. Methods of estimating spread velocity of human plague

Trend Surface Analysis (TSA)

Trend surface analysis of spatio-temporal dynamics of human plague spread can be divided into two steps[S2]. Firstly, we fit a polynomial model to build a trend surface. Here, the coordinates of the centres of the plague infected counties (latitude: x and longitude: y) were used to fit the time of plague firstly appearing in a county, in a polynomial model of order n based on least-squares regression.

The polynomial order, n, was chosen by increasing n one step at a time (from 1 to maximally 6) until failing to improve model fit significantly. A polynomial model of order 6 was selected, as it performed significantly better than models of order 1 to 5 (Table S1). Maximum 6 degree of polynomial regression was set as the highest degree by the software we used in this study, "spatial" package in R. The trend surface of the polynomial model of order 6 is shown in Figure S2. R-square of the polynomial model is 0.70.

Table S1. ANOVA results of polynomial models with degree from 1 to 6

N	*Res df*	Res Sum Sq	*df*	Sum Sq	F -value	*Pr(>F)*	*R*-Squared
1	538	453695					0.19
2	535	356114	3	97580	48.87	<0.001**	0.36
3	531	334109	4	22005	8.74	<0.001**	0.39
4	526	280738	5	53371	20.00	<0.001**	0.48
5	520	219271	6	61467	24.30	<0.001**	0.59
6	513	158139	7	61132	28.33	<0.001**	0.70

Secondly, partial differential equations (Δyear/ΔX andΔyear/ΔY) were derived from the fitted model, which allowed calculating the spread velocity along the longitude (v_x) and latitude (v_y) directions:

$$v_x = \frac{\partial x}{\partial year}, v_y = \frac{\partial y}{\partial year}$$

The vector sum of the two direction's velocities was the calculated plague spread

velocity[S2]:

$$v = \sqrt{\left(\frac{\partial x}{\partial year}\right)^2 + \left(\frac{\partial y}{\partial year}\right)^2}$$

The package "spatial" (version 7.3-3) under R statistical program (http://www.r-project.org/) environment was used to fit the TSA models (R version 2.13.1)[S3].

Figure S2. 3-D plot of trend surface of plague spread in China. X-axis: Longitude, Y-axis: Latitude, Z-axis: the year of plague firstly appearing (reversed by multiplying with -1 for easier view).

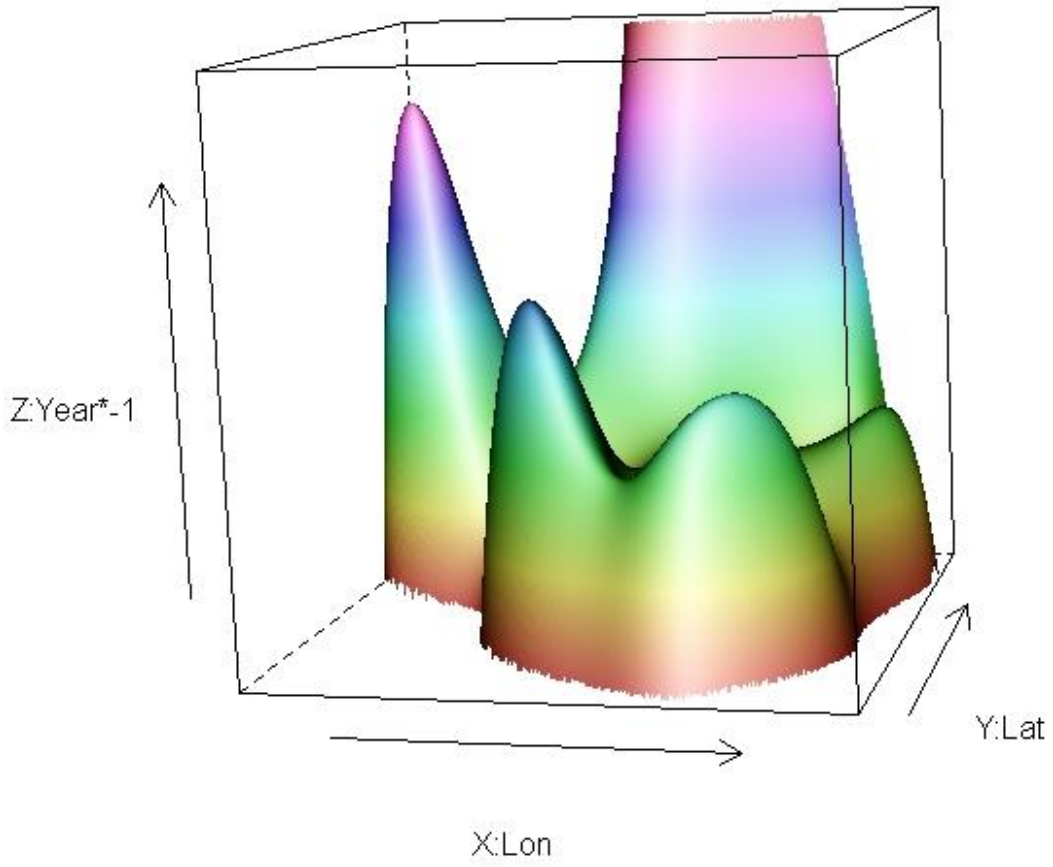

We also conducted Trend Surface Analysis with the degree of the polynomial regression above 6 (Fig. S3). These results indicate that degree higher than 6 does not improve model performance very much. Model performance was only little improved when the polynomial degree was higher than 6 (Fig. S3). Thus, polynomial degree of 6 was selected in this study.

Figure S3. Trend Surface Analysis with increase of degree in polynomial model above 6. Both AIC and R-squared are only moderately improved with increase of the polynomial degree above 6 (dashed line in the figure).

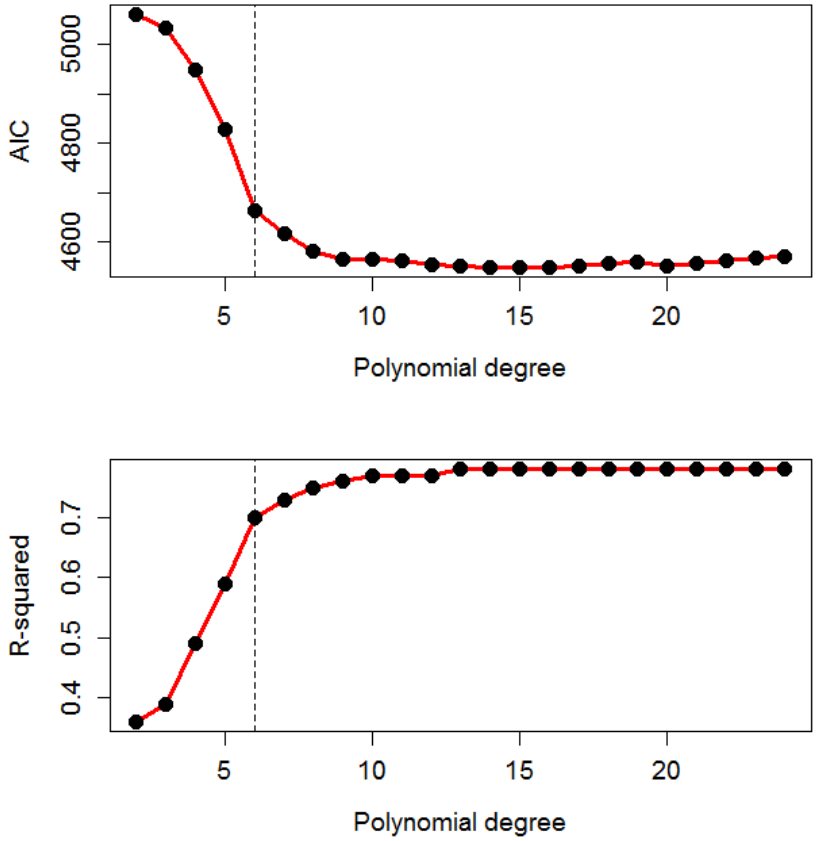

Nearest Neighbour Approach (NNA)

NNA works by following the principle of "earlier in time, then closest in space". We assumed that plague in a given county (sink county) was transmitted from the nearest county (source county) with first plague-invaded time (year) earlier than that of the sink county. That is, for a given sink county, we identified the source county as the county that was closest to the sink county in space among the counties having earlier first plague-invaded time (year) than the sink county.

Figure.S4. **Illustration of NNA in estimating the spread velocity of plague.** Consider three counties (C1, C2, C3) having first plague-invaded year of t1, t2 and t3 respectively. C1 and C2 are potential source counties to the sink county C3 because they have earlier plague-invaded time than C3. In panel A, for sink county C3, the source county is identified as C2, not C1, because C2 is closest to C3. In panel B, for the sink county C3, the source county is identified as C1, not C2 because C1 is closest to C3.

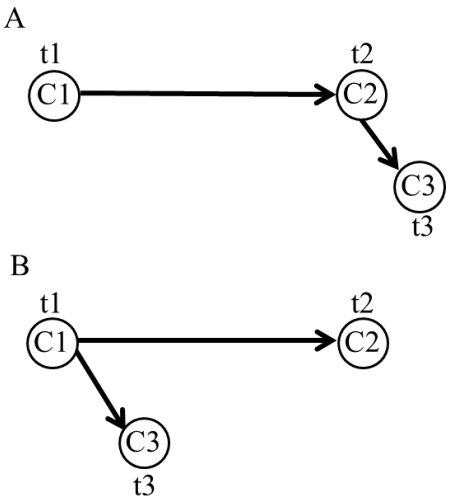

The R code to draw the transmission routes and to estimate the spread speed is attached below:

```
d <- function(x1,y1,x2,y2){
   v <- (I(x1-x2)^2 + I(y1-y2)^2)^0.5
   v}

for (i in 1:dim(data)[1]){
   data.i <- data[i,]
   year.i <- data.i$year
   if (data.i$year==min(data$year) {data$Speed.n[i] <- NA} ## Set the speed in the beginging of pandemics
   if (data.i$year> min(data$year)) {
      data.p <- data[data$year<year.i,]
      data.p$dis <- d(data.p$X,data.p$Y,rep(data.i$X,dim(data.p)[1]),rep(data.i$Y,dim(data.p)[1]))
         data.t <- data.p[order(data.p$dis),][1,]
         data$X.s[i] <- data.t$X; data$Y.s[i] <- data.t$Y ## output the coordinate of source county
         data$year.s[i] <- data.t$year
         data$Speed.n[i] <- data.t$dis/I(data.i$year-data.t$year) ## calculated the spread speed
         data$dis[i] <- data.t$dis ## output spread speed
   }
}
```

Sensitivity analysis of NNA to missing data.

Figure. S5. To test the sensitivity of NNA to the missing data, we present the transmission routes estimated by excluding 10% to 50% of the original plague-invaded counties randomly (Fig. S5). We found that the NNA appears to be highly robust to missing data in our study system, which may be related to the finding that each site has only very few connecting sites (Fig. S8). The basic transmission patterns estimated do not show much change in spite of missing data.

No missing data

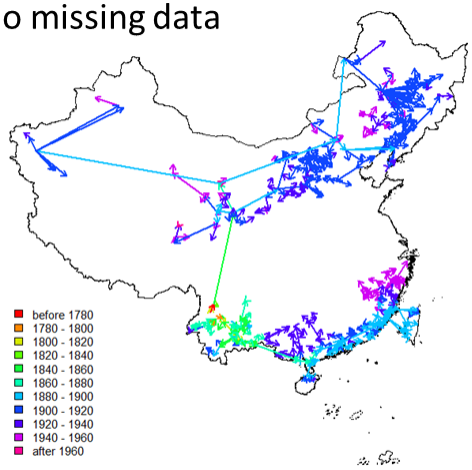

10% missing data

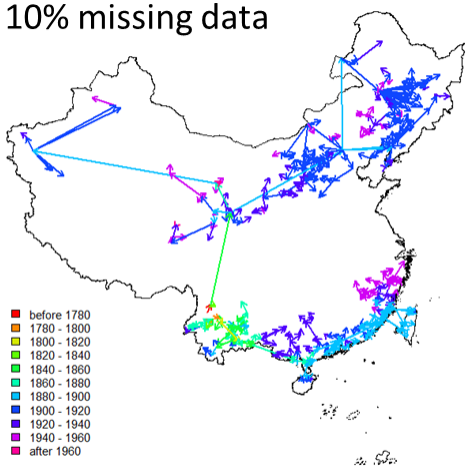

20% missing data

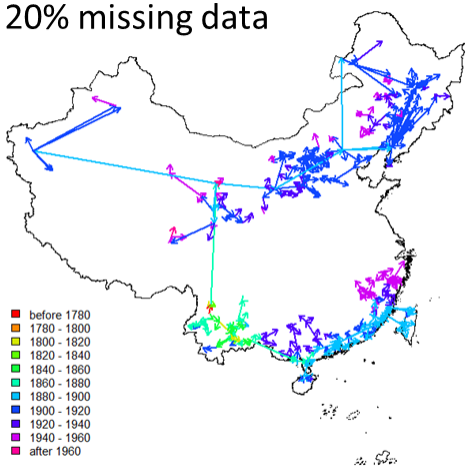

30% missing data

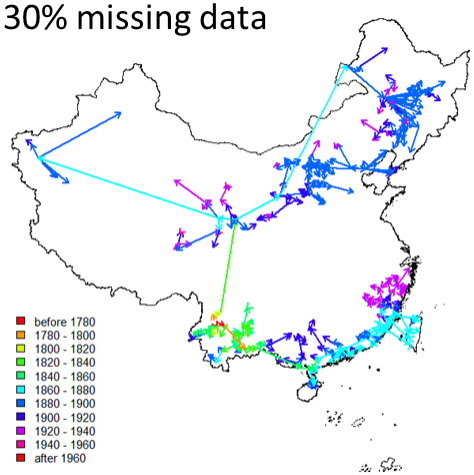

40% missing data

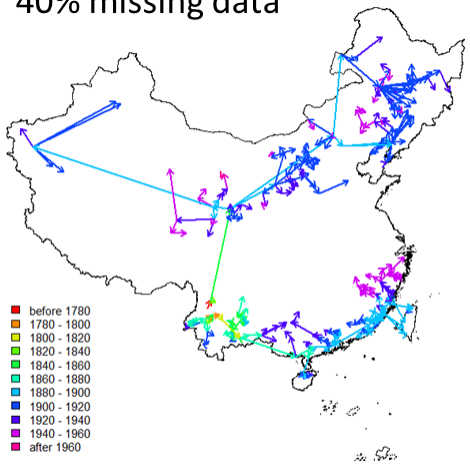

50% missing data

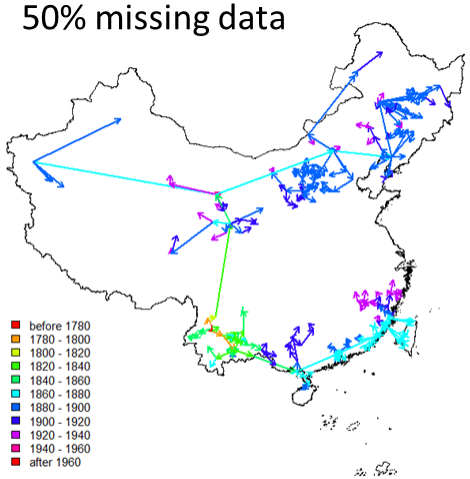

131

We used the Tukey multiple comparisons to identify significant differences of means of spread velocity with artificial missing data from 10-50% with that of the original data with no missing data. These results indicate that mean of spread velocity (log-transformed) of the original data with no missing data shows no significant difference with that of data with missing data of 10% (P = 1, n = 485), 20% (P = 0.99, n = 427), 30% (P = 0.96, n = 377) and 40% (P = 0.68, n = 319), but it shows significant difference with data with 50% missing data (P < 0.01, n =266).

Pearson correlation was conducted to test significant relationship between the original plague spread velocity (log-transformed) and that with 10% to 50% plague infected counties removed. Results indicated that original velocity is highly correlated with the velocity with missing data of 10% (r = 0.96, P < 0.01, $d.f.$ = 483), 20% (r = 0.93, P < 0.01, $d.f.$ = 425), 30% (r = 0.89, P < 0.01, $d.f.$ = 375), 40% (r = 0.85, P < 0.01, $d.f.$ = 317) and 50% (r = 0.71, P < 0.01, $d.f.$ = 264) (see Fig.S6). These results also indicate that NNA is highly robust to missing data.

Figure.S6. Scatterplot of the original plague spread velocity (log-transformed) and that with 10% to 50% plague infected counties removed. Black lines indicated the line y = x.

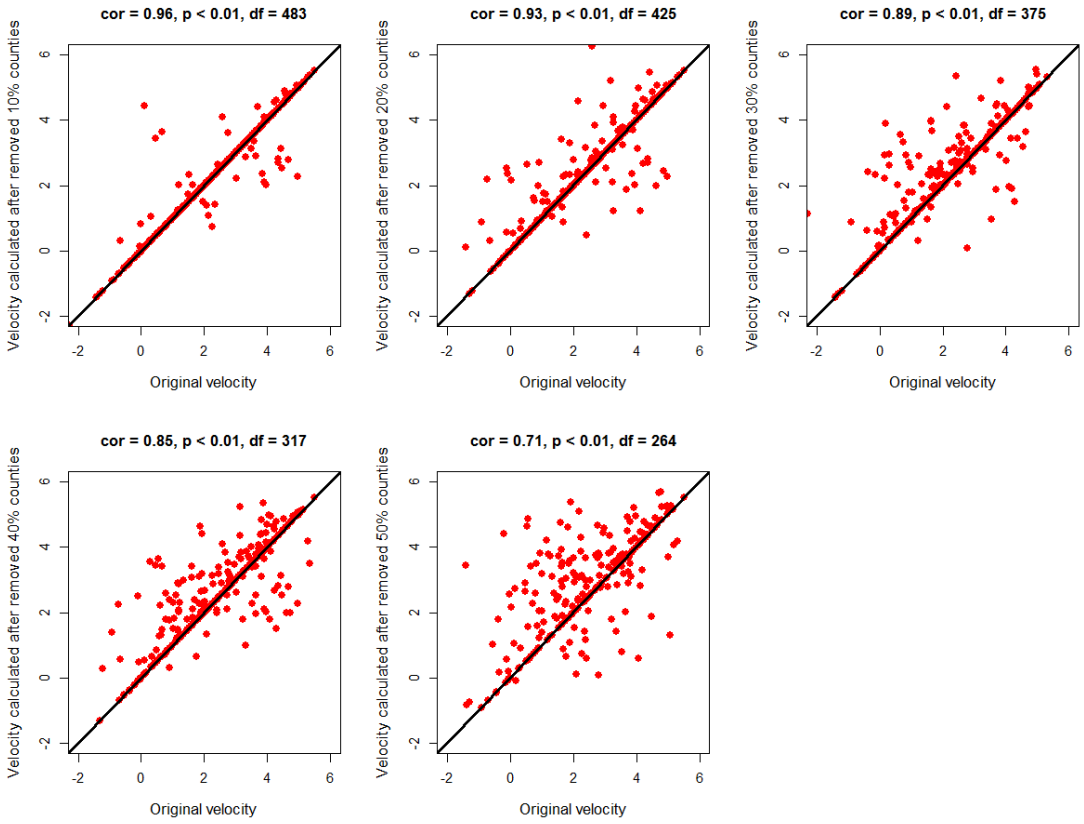

3. Spatial autocorrelations of spread velocity of human plague estimated by NNA and TSA

Figure S7. Estimated spread velocity of human plague from Trend-Surface Analysis (TSA) (A) and Nearest Neighbour Approach (NNA) (B). Each square shows the location of a county with recorded human plague. Colors of the squares indicate the estimated spread velocity. Please note that the velocity data were log-transformed. The TSA estimates of velocity are much more spatially autocorrelated than NNA estimates. Note: only regions with confirmed plague cases are shown. The spread velocity estimates from "source" to "sink" counties in (B) are plotted at the geographic coordinates of the sink counties.

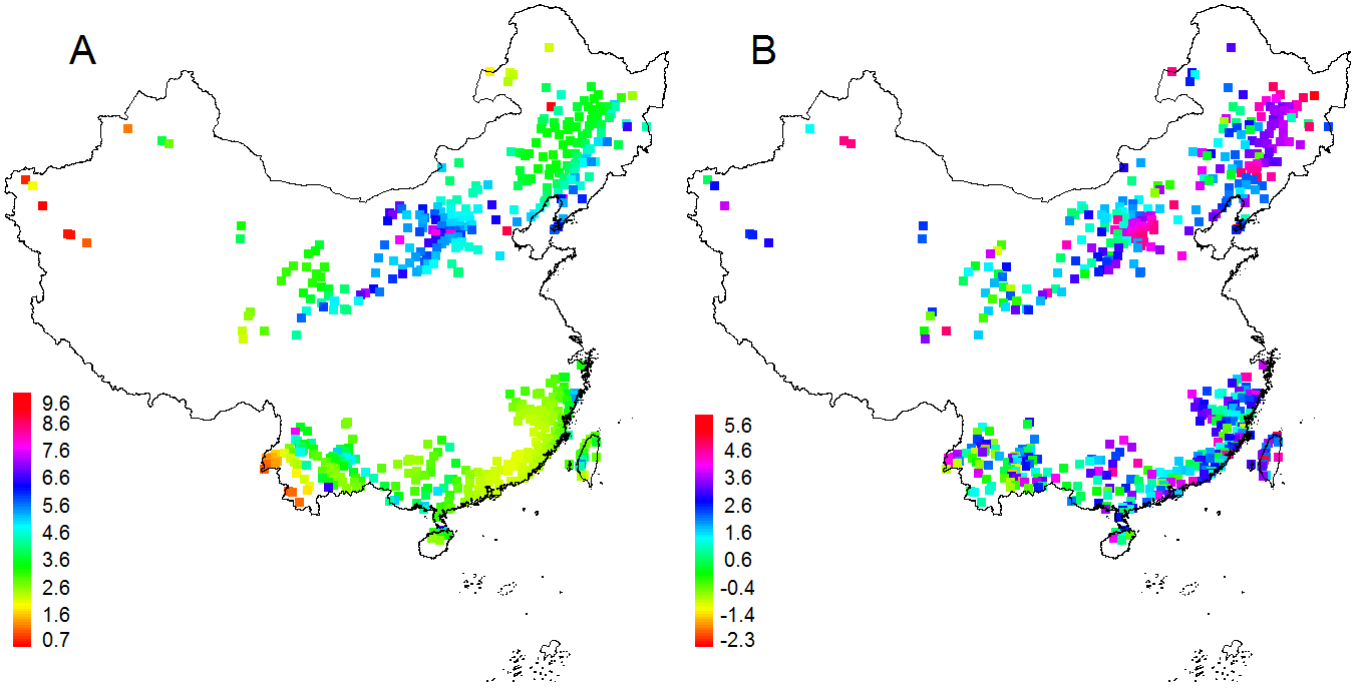

4. Estimation of the spread velocity of human plague

Here we present the quantiles, median and means of estimated plague spread velocity by using both TSA and NNA. We use a one-way ANOVA on log-transformed velocity values for TSA and NNA separately, to analyse the difference in the estimated velocity between North and South China. We found that plague spread significantly faster in North China (n = 257) than in South China (n = 283), according to both TSA ($F_{1,538}$ = 206.9, $p < 0.01$) and NNA ($F_{1,538}$ = 23.18, $p < 0.01$).

Table S2. The spread velocity of human plague in whole China, North China and South China estimated by NNA and TSA. Also see Fig. S8. Note that the velocity values were highly skewed before log-transformation, so that the mean at this scale is heavily influenced by a few extreme values.

Methods	Region	Plague spread velocity (ln (km/year))				Plague spread velocity (km/year)			
TSA		1st Qu.	Median	Mean	3rd Qu.	1st Qu.	Median	Mean	3rd Qu.
	Whole China	2.85	3.69	3.96	4.87	17.34	40.10	472.40	129.80
	South China	2.59	2.96	3.22	3.48	13.37	19.26	84.82	32.52
	North China	3.83	4.72	4.77	5.42	45.85	112.50	899.10	226.00
NNA	Whole China	1.32	2.47	2.42	3.64	3.72	11.76	28.41	38.12
	South China	1.02	2.24	2.13	3.28	2.77	9.42	21.19	26.69
	North China	1.68	2.74	2.74	3.91	5.35	15.50	36.35	50.11

Figure S8. Comparisons of the estimated spread velocities between using NNA and using TSA. The bold horizontal lines indicate the median. The bottom and top of the box indicate the 1st quantile and 3rd quantile. The dashed lines indicate the 95% confidence interval. Points outside of these intervals are defined as outliers (plotted as small circles).

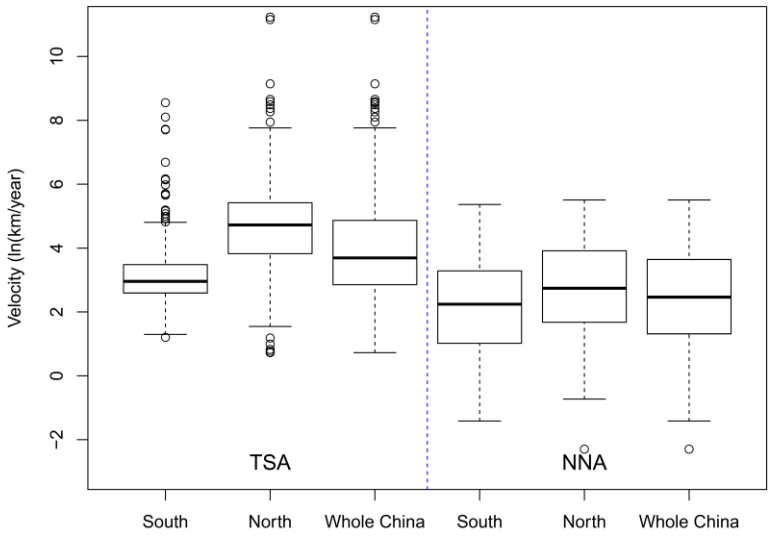

Accounting for difference in county area between North and South China

We calculated the average distance between the center of adjacent counties to each plague infected counties. We add this average distance in the ANOVA test to remove the potential effect of county area (average area of county is larger in the north than in the south) (Fig. S1).

The equation for the ANOVA test was:

Velocity of plague spread = binary variable indicating South China + average distance between neighbouring counties

Results still showed significantly faster plague spread in North China than in South China, according to both TSA ($F_{1,517} = 223.7$, $p < 0.01$) and NNA ($F_{1,517} = 29.89$, $p < 0.01$).

Figure S9. Frequency histogram of the estimated spread velocities by using NNA and TSA.

A: Histogram of the estimated spread velocities (log-transformed, same below) from whole China made by using the TSA method. Vertical broken lines show the mean value (same below). B: From North China by using TSA. C: From South China by using TSA. D: From whole China by using NNA. E: From North China by using NNA. F: From South China by using NNA.

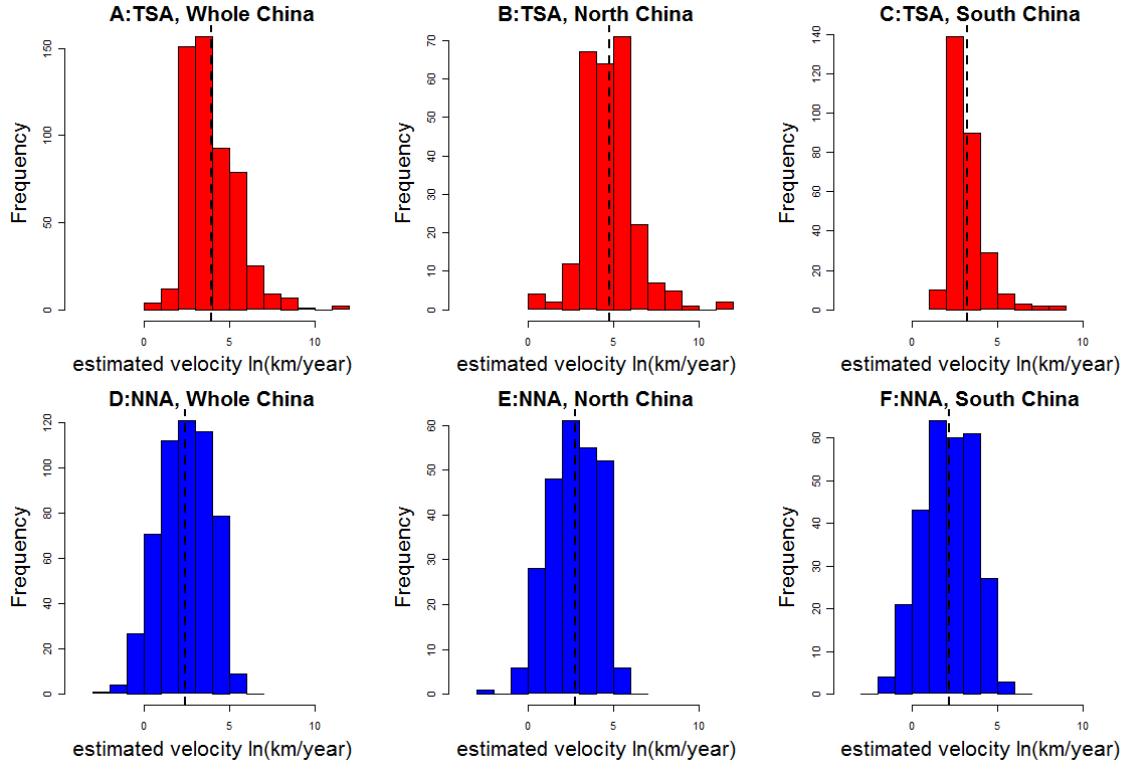

Figure S10 Frequency of transmission nodes (number of sink counties) per source county. This figure shows that the majority of source counties has only one or two sink counties.

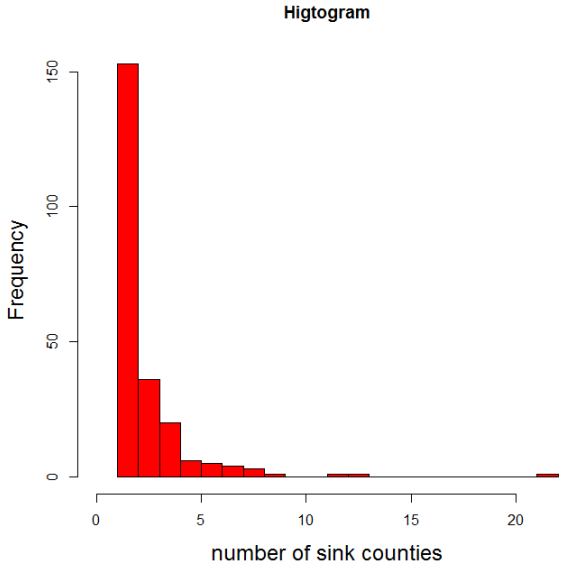

Figure S11. Time series of the estimated spread velocity of human plague in the whole China model by using TSA (top figure) and NNA (bottom figure) methods. We used boxplots to show the distribution of the estimated spread velocity within each year.

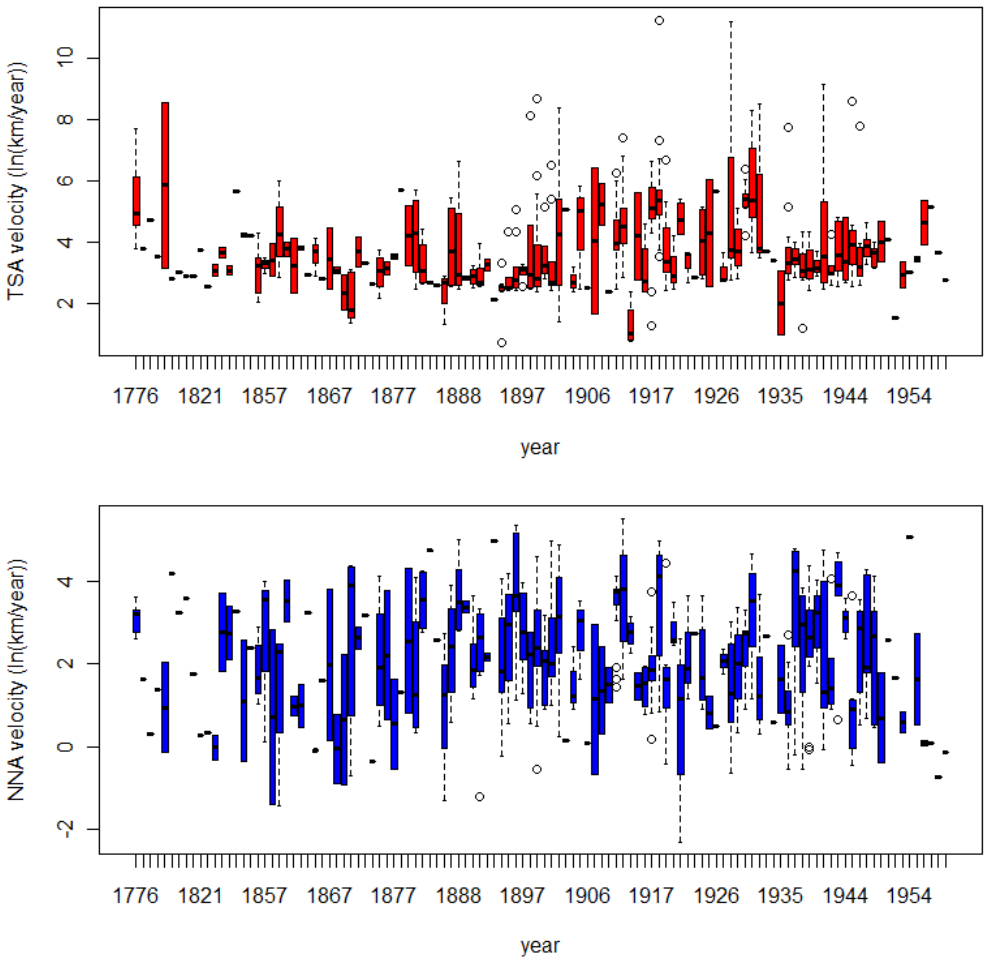

5. Effects of Dryness/wetness and transportation system including the ancient Silk Road and the Tea Road (*Chama Gudao*) on spread of plague in China

5.1 Dryness/wetness index

In the enormous amounts of Chinese historical records there are abundant climatic descriptions, which are of great value for studying climate fluctuations[S4]. The dryness/wetness index was constructed from these materials, including more than 2200 local annals and many other historical writings from the last 500 years[S4]. Statistical properties of this dryness/wetness index, for example consistency and persistency, have been carefully examined and established[S5]. An evaluation of the station networks and statistical techniques of dryness/wetness was made[S6]. Dryness/wetness variations in north China and the middle Yangtze River are confirmed by series of data on local precipitation and runoff [S7].

5.2 Comparison of the effects of dryness/wetness calculated for source and sink locations on spread velocity

We used the following model to look at climatic effects (as measured by dryness/wetness), with the dryness/wetness index referring to either sink or source locations.

$$V_{i,j} = a + b(Year_i) + c(Road_j) + d(River_j) + \mathrm{e}(Coast_j) + k(D/W_{i-1,j}) + \varepsilon_{i,j}$$

The definitions of smooth functions follow the METHODS section in the main text. Based on the results from the three models covering South, North and Whole China, we found that dryness/wetness at the source locations showed no significant effect on spread velocity.

Table S3. Comparisons of dryness/wetness (D/W) effect between sink and source locations

Region	Statistics	Effect of D/W at sink locations	Effect of D/W at source locations
South China			
	P-value of $k(D/W_{i-1,j})$ effects	*P < 0.01*	*P > 0.05*
	F	$F_{1.06,\ 7.73} = 13.02$	$F_{1.65,\ 11.9} = 2.52$
	GCV	*17.21*	*26.82*
North China			
	P-value of $k(D/W_{i-1,j})$ effects	*P < 0.01*	*P > 0.05*
	F	$F_{1,\ 67.36} = 22.165$	$F_{1.49,\ 8.87} = 0.4$
	GCV	*29.54*	*37.12*
Whole China			
	P-value of $k(D/W_{i-1,j})$ effects	*P < 0.01*	*P > 0.05*
	F	$F_{1.83,\ 9.24} = 32.0$	$F_{1.09,\ 11.7} = 0.03$
	GCV	*26.36*	*35.59*

5.3 Comparisons of the effects of road and climate on spread velocity of plague, using either the 1910 road map or the 1946 road map of China.

Because the transportation system has changed during the study period, we explored to which degree results change if we use a different road map than that used in the main analysis (i.e., for year 1910). Thus, we digitalized another available road map for 1946 and tested if roads still show significant effects on spread velocity of plague in China. 157 counties out of the 540 original counties (29.1%) showed changes of road locations from 1910 to 1946. Our modeling analysis indicates that roads, based on the 1946 map, show significant effect on plague spread (*Estimated increase in ln(velocity [km/year]* ± *standard error* = 0.31 ± 0.09, $t_{83.53}$ = 4.42, $P < 0.01$, n = 386), but the model performance (GCV = 15.79) is slightly worse than the original model in the main text (GCV = 15.3).

Using the 1946 road data[S8], we found that the effects of climate on spread velocity are similar to those using the 1910 road data in the main text (**Fig. S12**).

Figure. S12. Effects of dryness/wetness on spread velocity of plague using 1910 road data in South China (Panel **A**. $F_{1.6, 31.95}$ = 6.64, $p < 0.01$), North China (Panel **B**. $F_{1.82, 67.36}$ = 3.68, $p < 0.05$) and Whole China (Panel **C**. $F_{1, 82.56}$ = 17.41, $p < 0.01$); and using 1946 road data in South China (Panel **D**. $F_{1.86, 33.39}$ = 10.82, $p < 0.01$), North China (Panel **E**. $F_{1.77, 67.93}$ = 3.38, $p < 0.05$) and Whole China (Panel **F**. $F_{1, 83.53}$ = 17.14, $p < 0.01$).

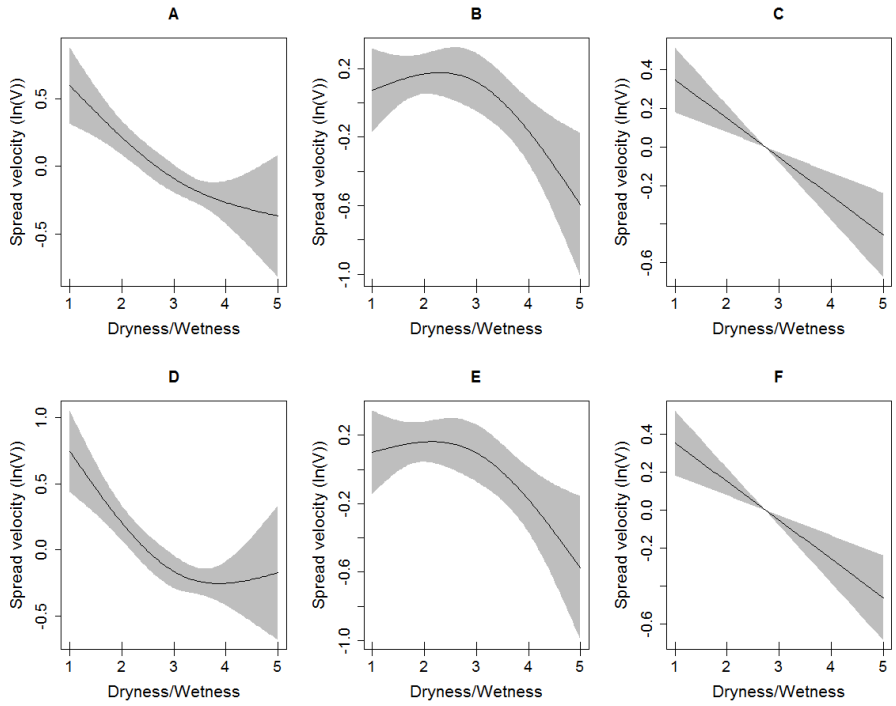

Figure S13. A. The road data extracted from the map published in 1946[S8]. Red lines indicate the major roads that were digitalized in this study. B. Plague infected counties with road (Red) and without road (Blue) passing through in the 1910 road map. C: Plague infected counties with road (Red) and without road (Blue) passing through in the 1946 road map.

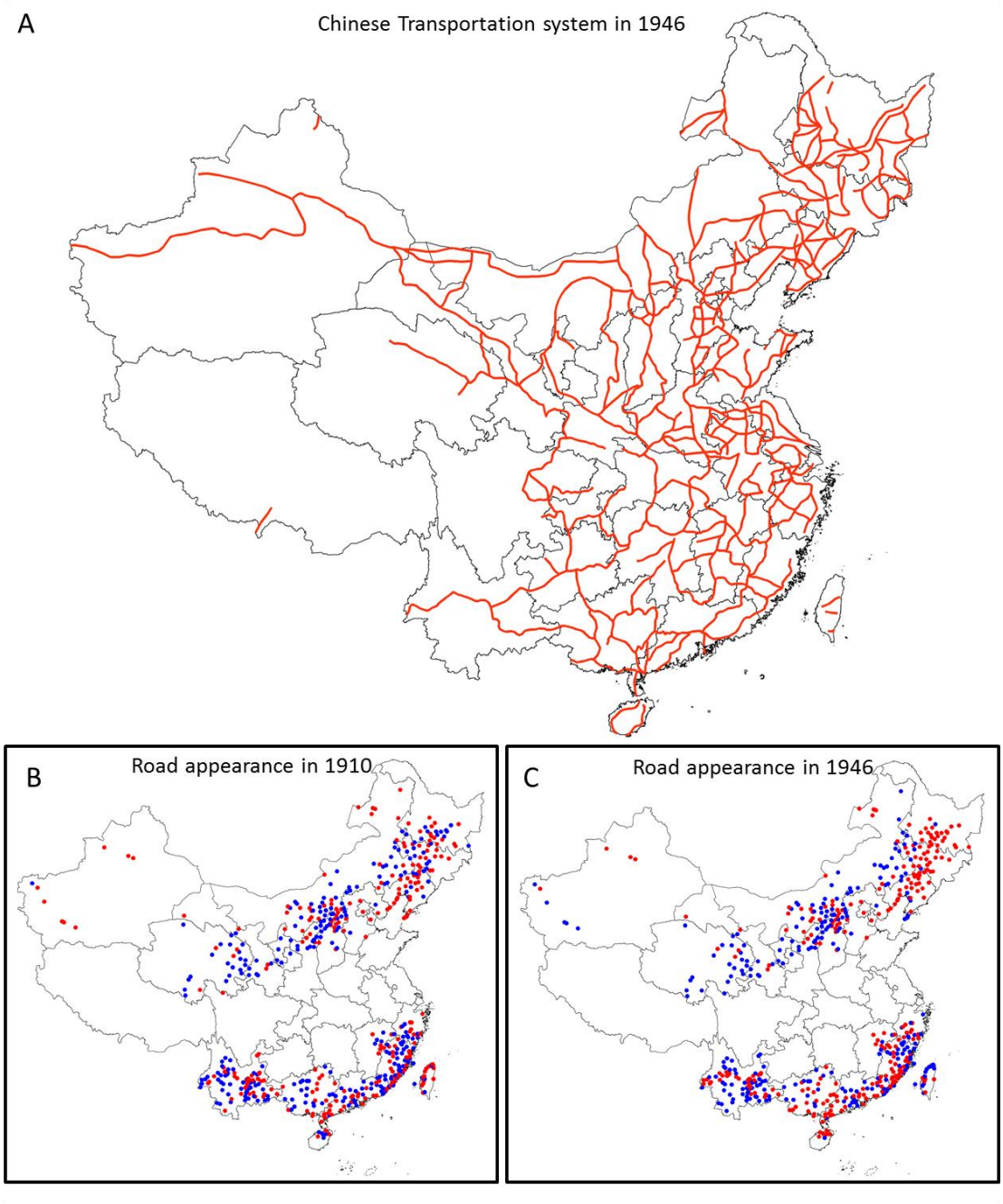

5.3 Map of ancient Tea Road (*Chama Gudao*) and Silk Road

The ancient Tea Road (*Chama Gudao* in Chinese, blue arrows in Fig. S14) is one of the oldest caravan route systems in Asia. In history, the Tea Road was a trade route from Yunnan, one of the tea-producing regions, to other provinces in China including Tibet, Sichuan, Qinghai and Gansu. The Tea Road was also linked to other countries, such as India and Nepal. The Tea Road had several branches. The red point marks Heqing county in Yunnan, the first county in which plague was found during the third pandemic. The green point is located in Tongren county of Qinghai, where the earliest case of plague was recorded in North China. The Tea Road may have played a key role in the long-distance spread of plague from Yunnan to North China (see Fig. 2 in the main text).

The Silk Road (red arrows in Fig. S14) refers to a network of interlinking trade routes across the Afro-Eurasian landmass that connected southern, eastern, and western Asia with the Mediterranean and parts of northern and eastern Africa, as well as Europe. These routes may have played a key role in the long-distance spread of plague to Xinjiang in western China (See Fig. 2 in the main text).

Figure S14. Map of the ancient Tea Road (*Chama Gudao*, blue arrows) and Silk Road (red arrows).

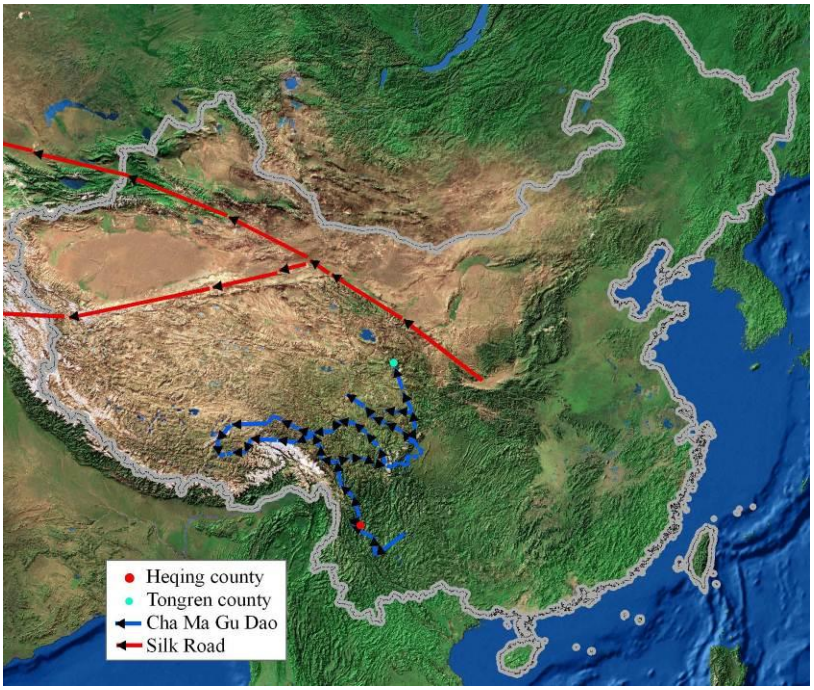

6. Model Construction and Selection

6.1. Models with and without interaction between location and plague prevalence

During model selection, we found that the inclusion of a location-dependent effect of plague prevalence was needed to reduce spatial correlation among the residuals, and that models with such a term were also favored in terms of GCV (Generalized Cross Validation). Here we present the results with and without the interaction.

We used a tensor-product anisotropic smooth function $k(Lon_j, Lat_j, Log(P_{i,j}))$ to quantify the interaction of plague prevalence with location on spread velocity. (For the definition of smooth functions, please see METHODS section in the main text). This tensor-product function was the interaction between a smooth function of log-transformed plague prevalence (cubic regression spline function with maximally 2 df) and a two-dimensional smooth function of longitude and latitude of the plague-invaded county (thin-plate regression spline with maximally 20 df).

We considered the following models:

Model S1 (with interaction)

$$V_{i,j} = a + b(Year_i) + c(Road_j) + d(River_j) + \mathrm{e}(Coast_j) + f(Ele_j) + g(Rug_j) + h(Lon_j, Lat_j, Log(P_{i,j})) + k(D/W_{i-1,j}) + \varepsilon_{i,j}$$

Model S2 (without interaction but with independent effects of plague prevalence and location)

$$V_{i,j} = a + b(Year_i) + c(Road_j) + d(River_j) + \mathrm{e}(Coast_j) + f(Ele_j) + g(Rug_j) + m(Lon_j, Lat_j) + n(Log(P_j)) + k(D/W_{i-1,j}) + \varepsilon_{i,j}$$

Model S3 (without interaction but with effect of location)

$$V_{i,j} = a + b(Year_i) + c(Road_j) + d(River_j) + \mathrm{e}(Coast_j) + f(Ele_j) + g(Rug_j) + m(Lon_j, Lat_j) + k(D/W_{i-1,j}) + \varepsilon_{i,j}$$

Model S4 (without interaction but with effect of plague prevalence)

$$V_{i,j} = a + b(Year_i) + c(Road_j) + d(River_j) + \mathrm{e}(Coast_j) + f(Ele_j) + g(Rug_j) + n(Log(P_j)) + k(D/W_{i-1,j}) + \varepsilon_{i,j}$$

The model selection results are shown in Table S3. Model S1 with interaction between plague prevalence and location had much lower GCV than models (Model S2-4)

without the interaction, especially for North China. Model diagnostics also indicated that Model S1 had lower spatial autocorrelation than the other models (see below).

Table S4. GCV of the tested models

Model area	GCV			
	Model S1	Model S2	Model S3	Model S4
South China	12.9*	13.5	13.9	16.0
North China	13.7*	21.9	22.3	27.6
Whole China	14.7*	17.6	18.0	25.8

*Model with lowest GCV of the four models.

6.2. Visualization of location-dependent effect of plague prevalence on spread velocity

As shown in Fig. S15, plague prevalence indeed interacts with location in affecting spread velocity. Black points indicate the plague-infected counties. If the effects of plague prevalence and location are independent as assumed in Model S2, the predicted spread velocity pattern in space should not change with a change of plague prevalence. However, we found that if we changed the plague prevalence from 4 to 8, the predicted spatial spread velocity pattern was greatly changed, indicating that there was strong interaction between plague prevalence and location in affecting spread velocity.

Figure S15. Visualized location-dependent effects of plague prevalence on spread velocity. Left figure: plague prevalence = 4 (equal to 55 human plague cases). Right figure: plague prevalence = 8 (equal to 2981 human plague cases). Counties with confirmed plague cases are shown in black points. Note: only plague-infected or related regions are shown.

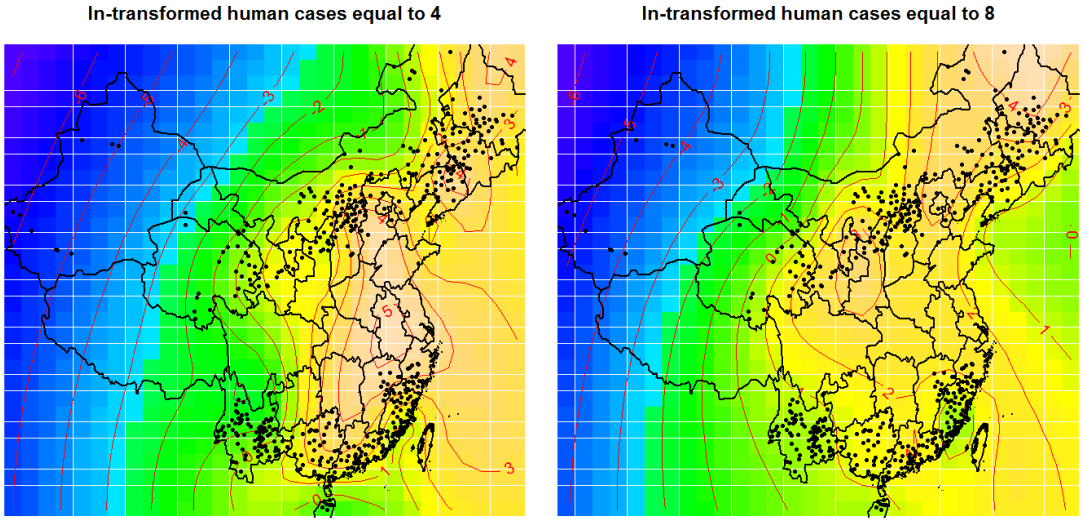

6.3. Results of models without interaction between location and plague prevalence

6.3.1. Results of model without the interaction (Model S2) in South China.

Figure S16. A: Smooth effect of Year ($F_{6.06,\ 26.8}$ = 2.67, p < 0.05). B: Smooth effect of the natural logarithm of the elevation ($F_{1.34,\ 26.8}$ = 0.18, p > 0.05). C: Smooth effect of the natural logarithm of the ruggedness ($F_{1,\ 26.8}$ = 0.006, p > 0.05). D: spatial smooth effects ($F_{11.63,\ 26.8}$ = 2.61, p < 0.01). E: Smooth effect of plague prevalence ($F_{1.48,\ 26.8}$ = 6.19, p < 0.01). F: Smooth effect of previous year's Dryness/Wetness ($F_{1.33,\ 26.8}$ = 3.67, p < 0.05). Model results on three binary predictor variables are listed as follows: road appearence (Estimated effect ± Std. Error: 0.69 ± 0.15, $t_{26.8}$ = 4.7, p < 0.01) , river appearance (-0.07 ± 0.16, $t_{26.8}$ = -0.4, p > 0.05) and coast appearence (0.47 ± 0.23, $t_{26.8}$ = 2.08, p < 0.05). Road and coastline showed significant and positive effects on spread velocity of human plague.

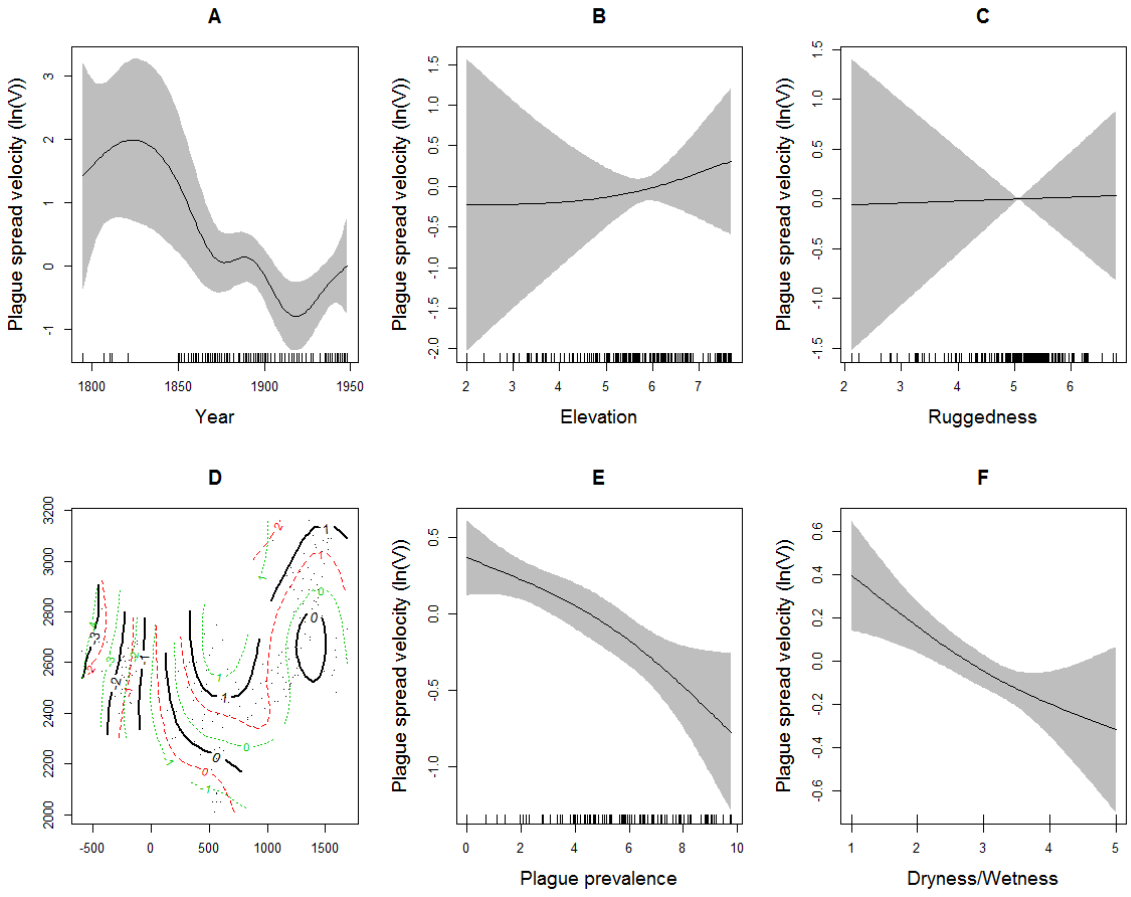

Figure S17. A: Autocorrelation function (ACF) of annual averages of residuals. B: Residual semi-variogram. These plots indicate whether there is any remaining temporal and/or spatial correlation in the residuals; for correctly specified models, these plots will not contain any systematic patterns, otherwise any systematic pattern may provide clues for further improvements of the model specification. ACF is useful for checking whether the residuals have any temporal structure. If there is no remaining residual spatial autocorrelation, the semivariogram should be approximately a flat line. In the presence of positive (negative) spatial autocorrelation, the semivariogram will tend to curve upwards (downward). Slight temporal autocorrlation of residuals may be due to stochastic effects.

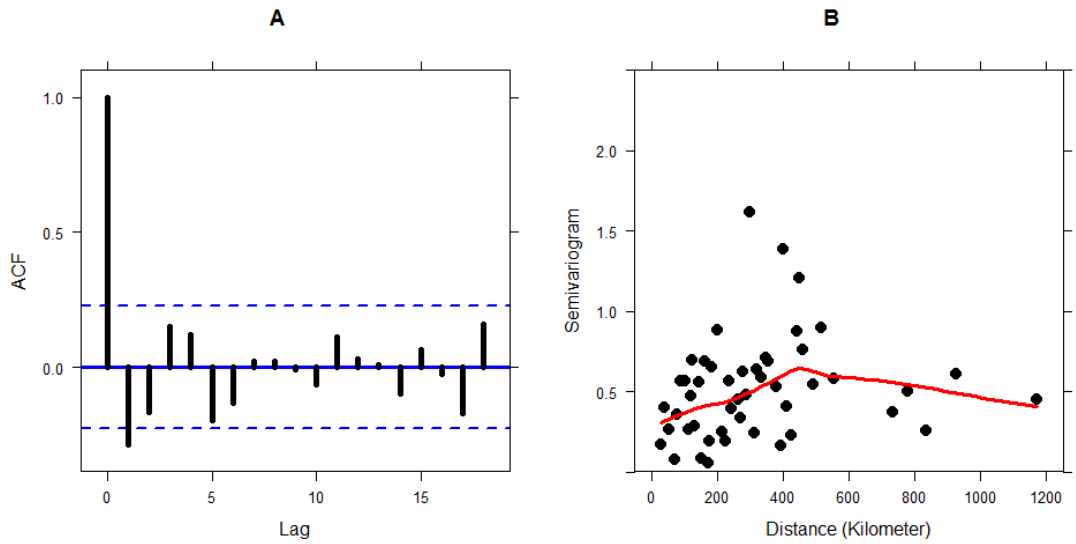

6.3.2. Results of model without the interaction (Model S2) in North China.

Figure S18. A: Smooth effect of Year ($F_{1,\ 25.8}$ = 19.34, p < 0.01). B: Smooth effect of the natural logarithm of the elevation ($F_{1,\ 25.8}$ = 3.94, p < 0.05). C: Smooth effect of the natural logarithm of the ruggedness ($F_{1,\ 25.8}$ = 2.45, p > 0.05). D: Spatial smooth effects ($F_{16.32,\ 25.8}$ = 3.63, p < 0.01). E: Smooth effect of plague prevalence ($F_{1.48,\ 25.8}$ = 4.26, p < 0.05). F: Smooth effect of previous year's Dryness/Wetness ($F_{1,\ 25.8}$ = 2.79, p > 0.05). Model results on three binary predictor variables are listed as follows: road appearence (Estimated effect ± Std. Error: 0.32 ± 0.11, $t_{25.8}$ = 2.83, p < 0.01) , river appearance (0.58 ± 0.13, $t_{25.8}$ = 4.44, p < 0.01) and coast appearance (-0.3 ± 0.49, $t_{25.8}$ = -0.611, p > 0.05). Road and river showed significant and positive effects on spread velocity of human plague.

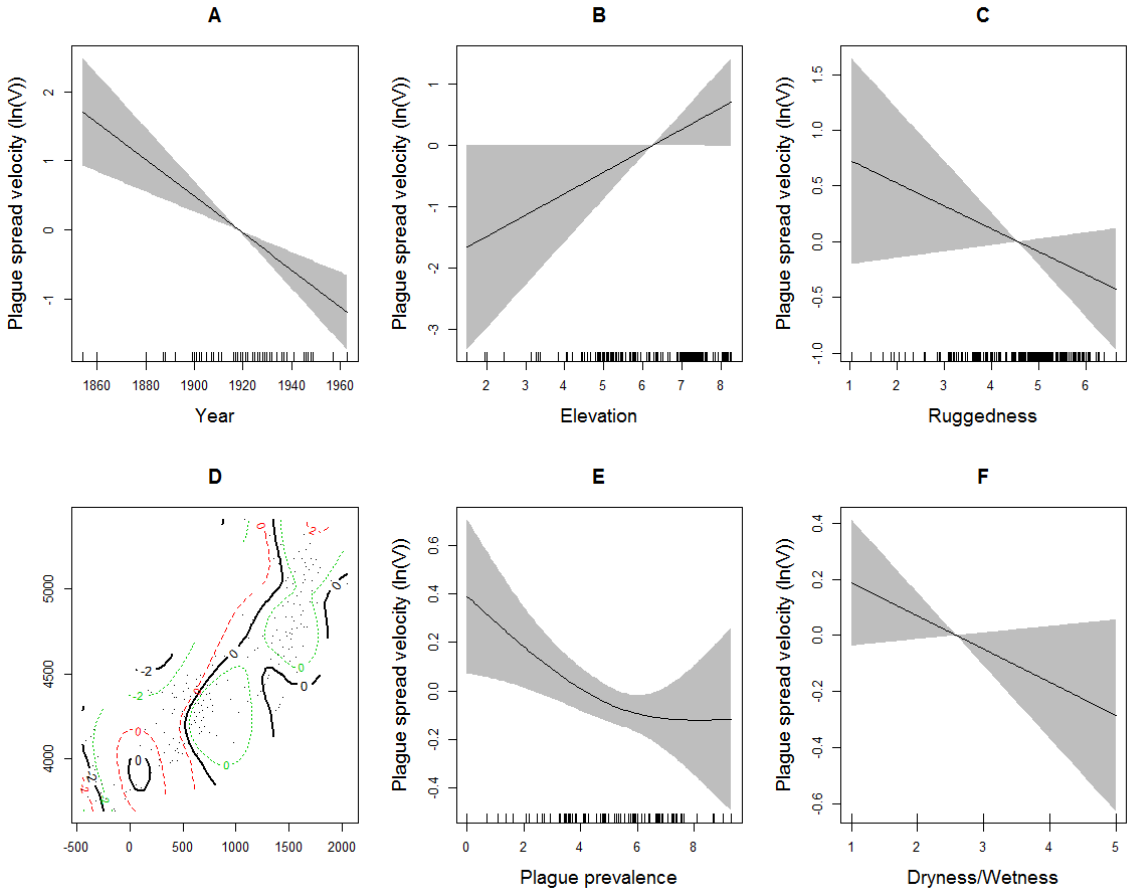

Figure S19. A: Autocorrelation function (ACF) of annual averages of residuals. B: Residual semi-variogram. See Figure S17 for interpretation of residual diagnostics plots.

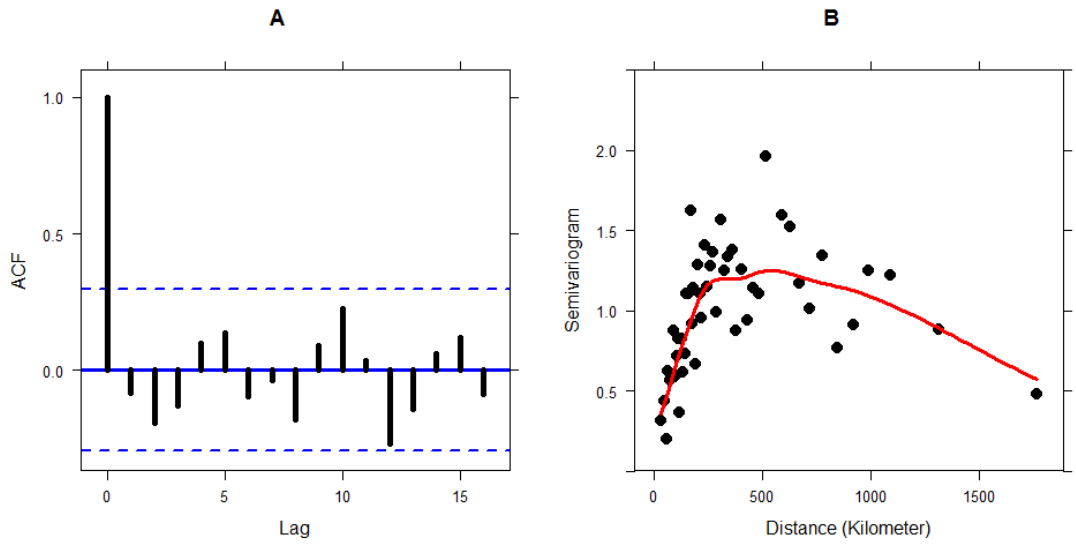

6.3.3. Results of model without the interaction (Model S2) for the whole China.

Figure S20. A: Smooth effect of Year ($F_{6.99, 45.06}$ = 6.21, p < 0.01). B: Smooth effect of the natural logarithm of the elevation ($F_{1.82, 45.06}$ = 5.83, p < 0.01). C: Smooth effect of the natural logarithm of the ruggedness ($F_{2, 45.06}$= 3.63, p < 0.05). D: Spatial smooth effects ($F_{28.07, 45.06}$= 6.93, p < 0.01). E: Smooth effect of plague prevalence ($F_{1.18, 45.06}$ = 14.13, p < 0.01). F: Smooth effect of previous year's Dryness/Wetness ($F_{1, 45.06}$= 10.1, p < 0.01). Model results on three binary predictor variables are listed as follows: road appearence (Estimated effects ± Std. Error: 0.38 ± 0.09, $t_{45.06}$ = 4.43, p < 0.01), river appearance (0.38 ± 0.1, $t_{45.06}$ = 4, p < 0.01) and coast appearance (0.57 ± 0.21, $t_{45.06}$ = 2.75, p < 0.01). Road, river and coastline showed significant and positive effects on spread velocity of human plague.

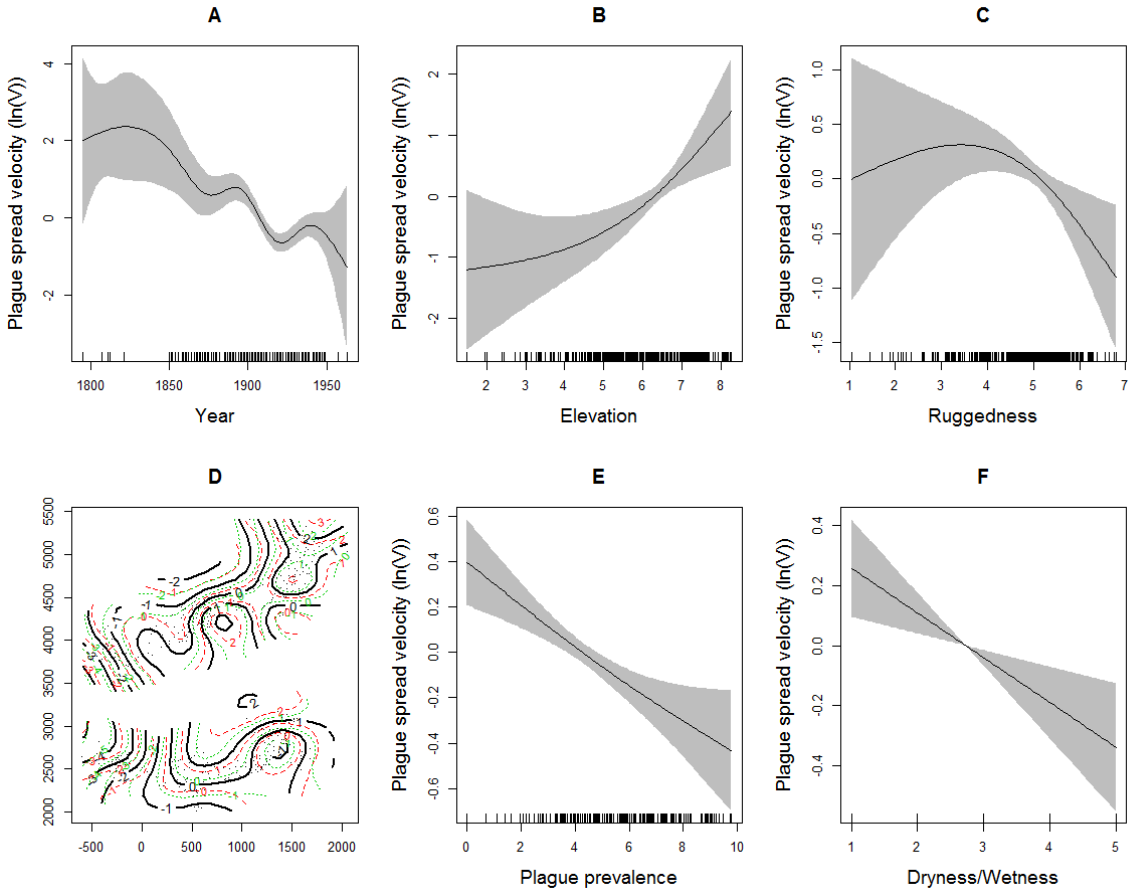

Figure S21. A: Autocorrelation function (ACF) of annual averages of residuals. B: Residual semi-variogram. See Figure S17 for interpretation of residual diagnostics plots.

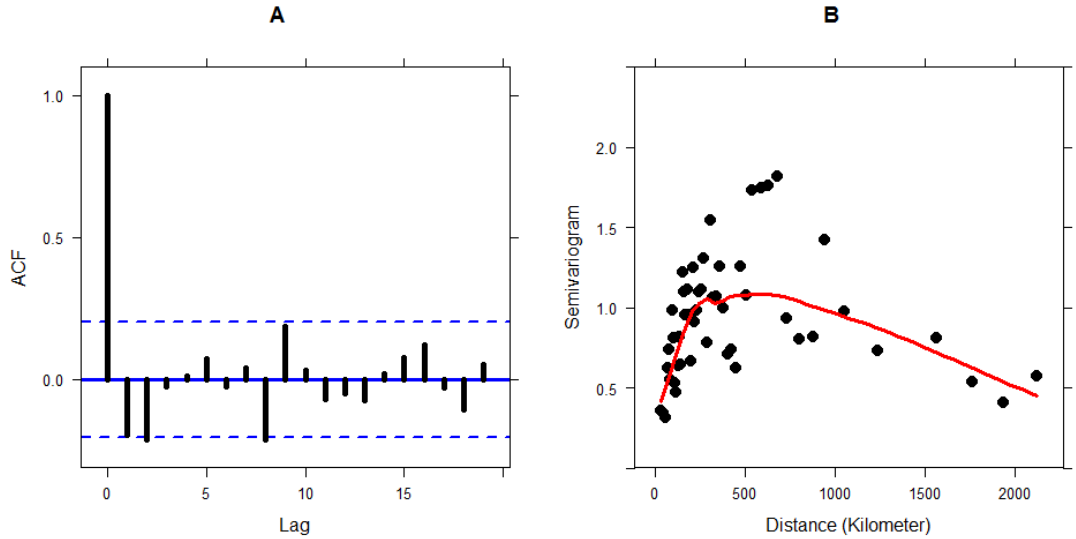

6.4. Results of models with interaction between location and plague prevalence

6.4.1. Model selection

Table S5. Model selection using GCV

We used stepwise backward selection based on GCV criterion. Models with lower GCV have higher out-of-sample predictive power, and are hence preferred. Terms were dropped one by one until the model formulation providing the lowest GCV was found.

Deleted factors	Backward Model selection steps				
	1	2	3	4	5
South China	GCV	GCV	GCV	GCV	GCV
Full model	12.9				
$b(Year_i)$	13.7	13.6	13.6	13.6	14.0(*)
$c(Road_j)$	14.3	14.2	14.1	13.9	14.2
$d(River_j)$	12.8*				
$e(Coast_j)$	13.3	13.2	13.0	12.9(*)	
$f(Ele_j)$	13.0	12.8	12.7**		
$g(Rug_j)$	12.9	12.7*			
$I(Loc_i, Loc_j, Log(d_{i,j}))$	17.2	17.0	17.2	17.0	17.2
$k(D/W_{t-1,j})$	17.8	17.8	18.0	18.4	18.4
North China					
Full model	13.7				
$b(Year_i)$	20.1	20.0	21.2	21.0	
$c(Road_j)$	13.9	13.8(*)			
$d(River_j)$	14.1	14.0	14.1	14.2 (*)	
$e(Coast_j)$	13.6**				
$f(Ele_j)$	14.8	14.6	14.6	15.3	
$g(Rug_j)$	14.2	14.0	14.1 (*)		
$I(Loc_i, Loc_j, Log(d_{i,j}))$	28.1	29.1	29.3	29.0	
$k(D/W_{t-1,j})$	18.9	18.7	19.7	19.5	
Whole China					
Full model	18.4				
$b(Year_i)$	19.9	19.8	19.8	19.8	
$c(Road_j)$	19.6	19.5	19.4	19.4	
$d(River_j)$	19.0	18.9	18.8	18.8(*)	

$e(Coast_j)$	18.4	18.3	18.3(*)	
$f(Ele_j)$	18.3*			
$g(Rug_j)$	18.3	18.2**		
$h(Lon_j, Lat_j, Log(P_{i,j}))$	26.5	26.5	26.4	26.4
$k(D/W_{i-1,j})$	22.0	22.0	22.1	22.0

*GCV reduced by omission of term

** final model.

(*) Omission of term(s) led to no further reduction in GCV

The final selected models with interactions are list below:

South China

$$V_{i,j} = a + b(Year_i) + c(Road_j) + e(coast_j) + h(Lon_j, Lat_j, \mathrm{Log}(P_{i,j})) + k(D/W_{i-1,j}) + \varepsilon_{i,j}$$

North China

$$V_{i,j} = a + b(Year_i) + c(Road_j) + d(River_j) + f(Ele_j) + g(Rug_j) + h(Lon_j, Lat_j, \mathrm{Log}(P_{i,j})) + k(D/W_{i-1,j}) + \varepsilon_{i,j}$$

Whole China

$$V_{i,j} = a + b(Year_i) + c(Road_j) + d(River_j) + e(Coast_j) + h(Lon_j, Lat_j, \mathrm{Log}(P_{i,j})) + k(D/W_{i-1,j}) + \varepsilon_{i,j}$$

6.4.2 Results of the South China model

Figure S22. Effects of predictor variables in the South China model.

A: Smooth effect of year ($F_{5.6,\ 31.95}$ = 2.83, p < 0.01). B: Smooth effect of previous year's Dryness/Wetness ($F_{1.6,\ 31.95}$ = 6.64, p < 0.01).

In addition, the model included one spatial term: spatially-variable effect of previous plague prevalence ($F_{21.74,\ 31.95}$ = 3, p < 0.01) and two binary predictor variables: road appearence (Estimated effect 0.63 ± 0.14, $t_{31.95}$ = 4.49, p < 0.01) and coast appearance (0.38 ± 0.2, $t_{31.95}$ = 1.94, p = 0.054, p < 0.1).

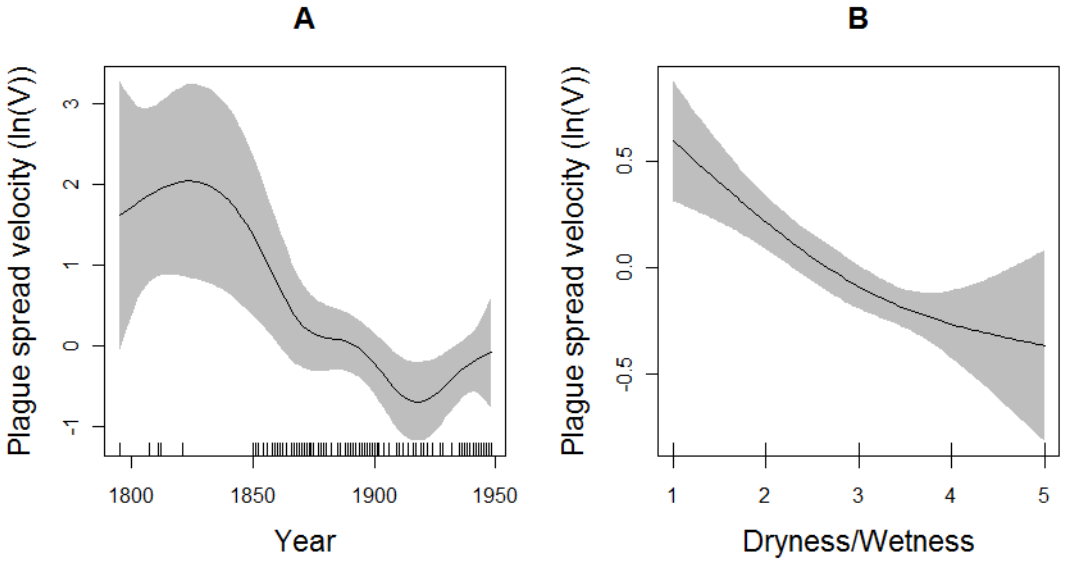

Figure S23. Residual diagnostics for the South China model.

A: Autocorrelation function (ACF) of annual averages of residuals. B: Residual semivariogram. See Figure S17 for interpretation of residual diagnostics plots.

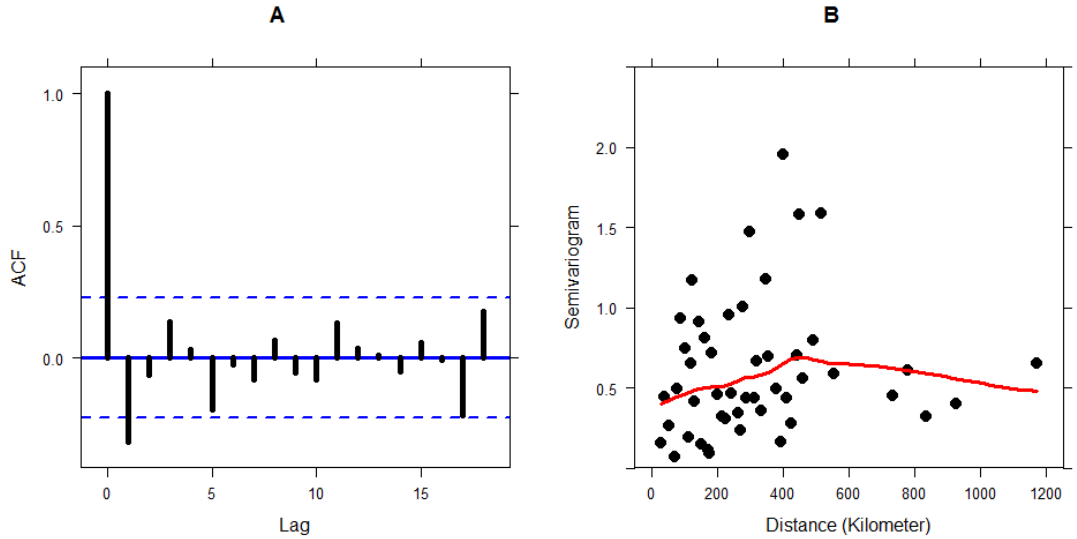

6.4.3 Results of the North China model

Figure S24. Effects of predictor variables in the North China model.

A: Smooth effect of Year ($F_{8.88,\ 67.36}$ = 7.54, p < 0.01). B: Smooth effect of the natural logarithm of the elevation ($F_{1,\ 67.36}$ = 12.34, p < 0.01). C: Smooth effect of the natural logarithm of the ruggedness ($F_{1.54,\ 67.36}$ = 3.96, p < 0.05). D: Smooth effect of previous year's Dryness/Wetness ($F_{1.83,\ 67.36}$ = 3.68, p < 0.05).

In addition, the model included one spatial term: spatially-variable effect of previous plague prevalence ($F_{51.12,\ 67.36}$ = 5.89, p < 0.01). Two binary predictor variables: road appearance (Estimated effect 0.22 ± 0.1, $t_{67.36}$ = 2.3, p < 0.05) and river appearance (0.29 ± 0.12, $t_{67.36}$ = 2.46, p < 0.05) were found to significantly affect plague spread velocity.

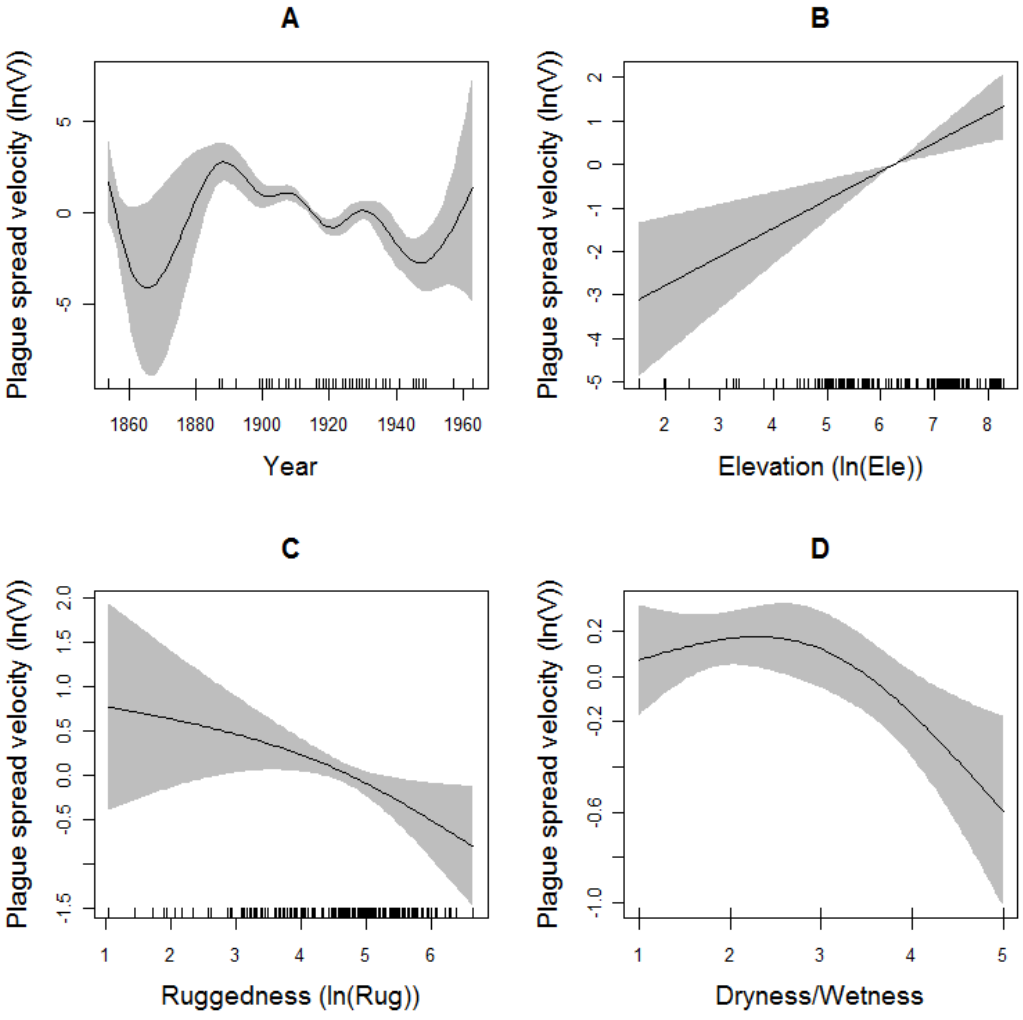

Figure S25. Residual diagnostics for the North China model.

A: Autocorrelation function (ACF) of annual averages of residuals. B: Residual semi-variogram. See Figure S17 for interpretation of residual diagnostics plots.

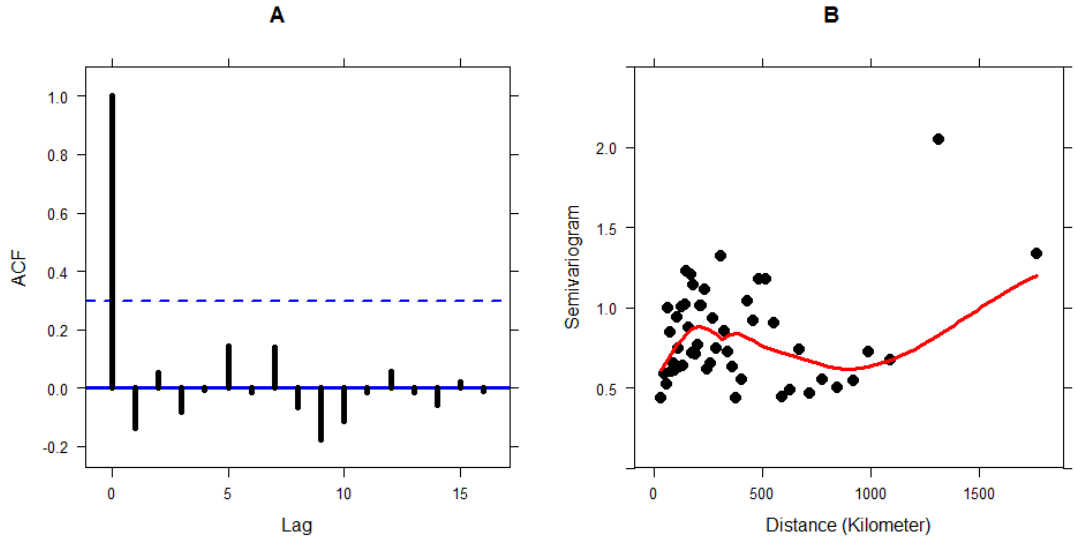

6.4.4 Results of the Whole China model

Because the Whole China model cover regions of both North and South, we increased the degree of freedom from 20 to 30 in two-dimensional smooth function of longitude and latitude of plague invaded county in tensor-product anisotropic smooth function. Model diagnostic also revealed that the increase of spatial degree of freedom reduced spatial autocorrelation (See Fig. S27).

Figure S26. Effects of predictor variables in the Whole China model.

A: Smooth effect of year ($F_{8.79,\ 82.56}$ = 6.92, p < 0.01). B: Smooth effect of previous year's Dryness/Wetness ($F_{1,\ 82.56}$ = 17.41, p < 0.01).

In addition, the model included one spatial term: spatially-variable effect of previous plague prevalence ($F_{68.77,\ 82.56}$ = 4.9, p < 0.01). Three binary predictor variables: road appearence (Estimated effect 0.38 ± 0.08, $t_{82.56}$ = 4.7, p < 0.01), river appearance (Estimated effect 0.2 ± 0.09, $t_{82.56}$ = 2.13, p < 0.05) and coast appearance (Estimated effect 0.44 ± 0.19, $t_{82.56}$=2.34, p < 0.05) were found to significantly affect plague spread velocity.

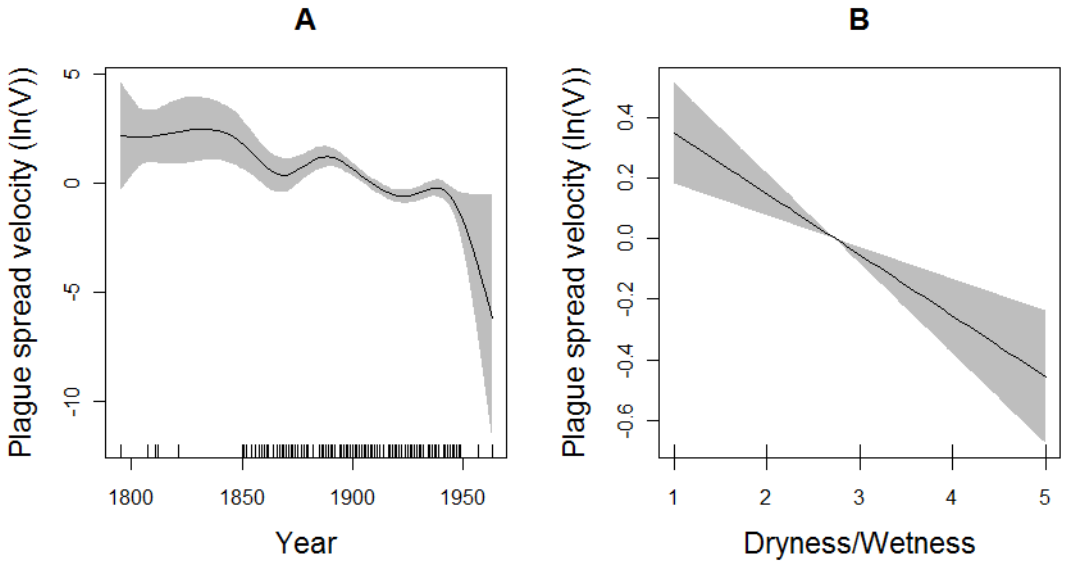

Figure S27. Residual diagnostics for the Whole China model.

A: Autocorrelation function (ACF) of annual averages of residuals with the model of the higher spatial degree of freedom (*df* = 30). B: Residual semi-variogram. C: Autocorrelation function (ACF) of annual averages of residuals with the model of the lower spatial degree of freedom (*df* = 20). D: Residual semi-variogram. See Figure S17 for interpretation of residual diagnostics plots.

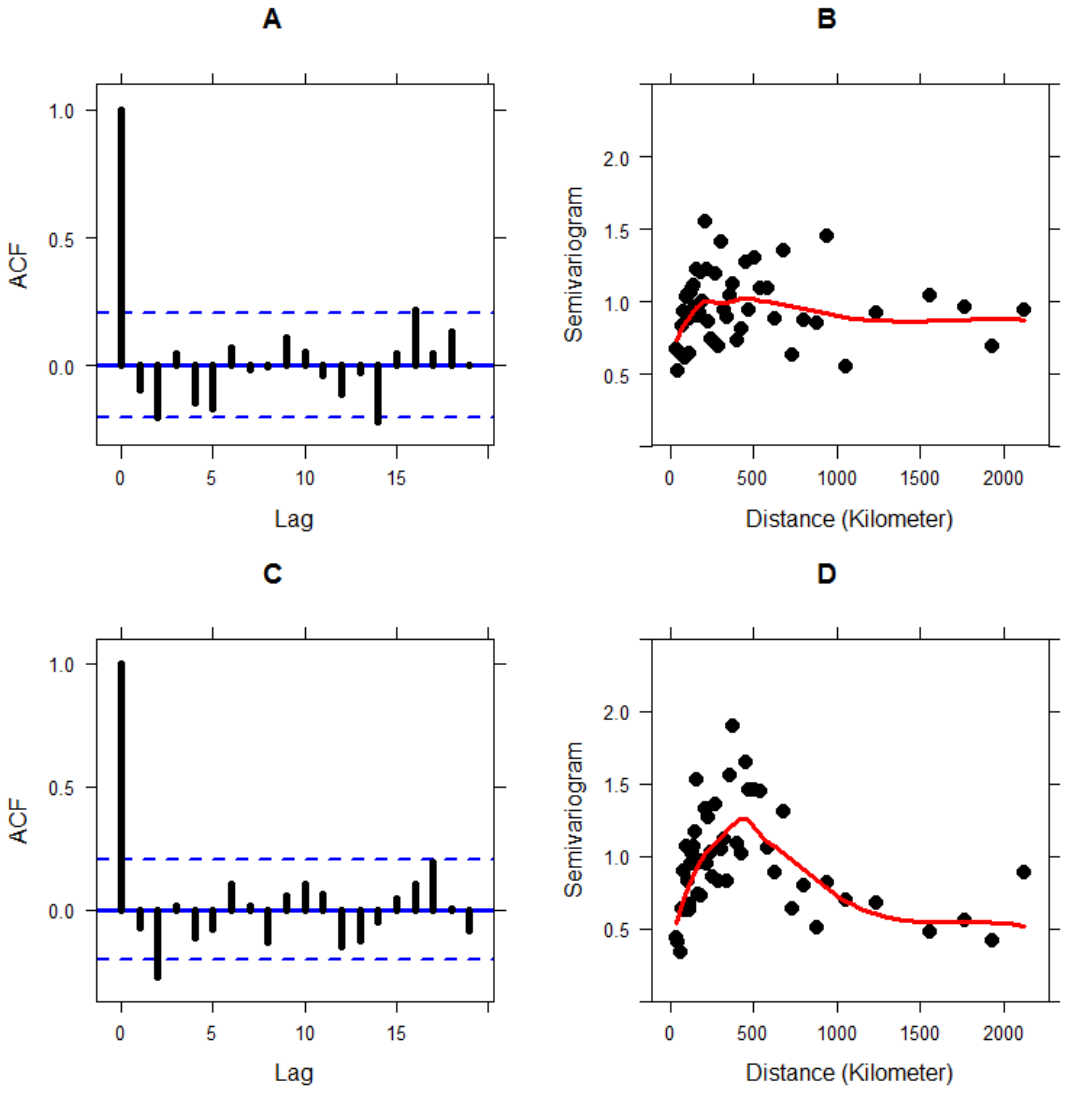

458 **References**

459 S1. Institute of Epidemiology and Microbiology, Chinese Academy of Medical
460 Sciences (1980) *The History of Spread of Plague in China*, pp 33-1794 (in
461 Chinese).

462 S2. Adjemian J Z, Foley P, Gage K L & Foley J E (2007) Initiation and spread of
463 travelling waves of plague, *Yersinia pestis*, in the western united states. *Am J*
464 *Trop Med Hyg* 76: 365-375.

465 S3. R Development Core Team (2006) *R: A Language and Environment for Statistical*
466 *Computing* (R Foundation Stat Comput, Vienna).

467 S4. Central Meteorological Bureau 1981 *Yearly Charts of Dryness/Wetness in China*
468 *for the Last 500-Year Period*. Cartographic Publishing House, Beijing.

469 S5. Yao C.S. 1982. A Statistical Approach to Historical Records of Flood and Drought.
470 *J Appl Meteorol*, 21: 588-594.

471 S6. Ronberg B. & Wang W. C. 1987. Climate Patterns Derived from Chinese Proxy
472 Precipitation Records - an Evaluation of the Station Networks and Statistical
473 Techniques. *J Climatol*, 7, 391-416.

474 S7. Qian W., Chen D., Zhu Y. & Shen H. 2003. Temporal and spatial variability of
475 dryness/wetness in China during the last 530 years. *Theor Appl Climatol*, 76,
476 13-29.

477 S8. Yang J. X. & Li Q. C. 1946. *Map of China*. Huan Cheng Press, Shanghai.

478

Data

Coordinates (x, y) of plague invaded counties and the year of plague firstly appeared

x	y	year	x	y	year	x	y	year
100.1743	26.56242	1772	116.3476	23.54034	1899	111.492	39.4404	1918
99.94741	26.11001	1776	119.5322	26.19938	1900	114.2305	39.43898	1918
100.0831	25.98794	1776	110.9847	37.95877	1900	112.4559	39.98689	1918
100.5742	25.82995	1776	121.7435	24.76049	1900	112.7202	38.72762	1918
100.2214	25.59046	1776	120.8165	24.56672	1900	113.2513	38.72288	1918
100.3125	25.58463	1776	112.2241	22.69757	1900	112.3215	37.3535	1918
100.3076	25.23076	1776	109.6809	19.90993	1900	98.47551	36.93175	1919
100.233	26.87601	1779	117.1804	23.70913	1901	123.308	44.1264	1919
100.4855	25.34738	1792	117.3345	23.95887	1901	116.3829	37.62452	1919
101.2393	25.51043	1795	117.4238	23.69832	1901	111.5245	23.23659	1919
99.90135	26.53248	1803	122.2269	40.67217	1901	114.4852	24.37268	1919
101.5448	25.03646	1803	111.9731	43.65241	1901	110.0977	19.36501	1919
103.4014	23.36832	1807	113.0273	23.71052	1901	102.3969	22.99721	1919
102.4907	23.71751	1811	116.1744	23.76346	1901	119.3333	27.10813	1920
102.8239	23.61798	1812	86.21672	44.30162	1901	123.724	50.5863	1920
102.7587	24.11184	1820	86.89809	44.18492	1901	122.7384	48.00245	1920
100.7455	26.68945	1821	119.1586	48.78391	1902	121.2737	38.81717	1921
99.90995	24.59824	1833	121.9957	46.01028	1902	127.9615	45.21479	1921
101.2725	25.19453	1848	111.1485	40.27731	1902	129.3833	44.57312	1921
102.4013	24.17753	1848	108.6525	40.7207	1902	131.1171	44.05932	1921
102.4859	24.92375	1850	110.8718	39.64355	1902	118.1152	27.33132	1922
103.7961	25.49455	1850	111.1207	38.46533	1902	121.7638	42.72964	1922
102.5428	24.35727	1851	109.2953	22.42456	1902	120.6551	42.8449	1922
102.5927	24.67158	1851	112.4315	23.63673	1902	95.80061	34.13261	1923
103.6642	25.0314	1852	75.99867	39.45944	1902	119.5426	26.49081	1924
102.0108	35.51421	1854	100.7036	23.50066	1902	118.5327	27.92099	1924
101.1004	25.85613	1854	99.93166	22.56223	1902	122.1578	39.40146	1924
103.254	25.56282	1855	102.5105	35.19759	1903	99.58253	32.88549	1924
100.9721	22.78349	1856	118.7386	26.58053	1904	117.8033	26.79756	1925
101.0425	23.06404	1856	115.7693	23.92254	1904	108.8027	37.59456	1925
100.8321	24.45229	1856	110.0055	19.73477	1904	110.4893	38.02248	1926
103.4421	24.40668	1856	102.4966	34.58817	1905	118.8513	27.36931	1927
104.6994	23.12599	1856	119.4343	49.3227	1905	118.9812	26.91349	1927
102.9162	24.6734	1856	108.1801	37.24301	1905	122.3496	42.94922	1927
102.7441	23.16502	1857	113.3759	22.64285	1906	118.7784	27.5281	1928
104.2435	23.37147	1857	109.7358	39.57232	1907	119.462	25.96684	1928
104.672	23.44082	1857	98.58643	24.44153	1907	101.4279	36.04206	1928
100.5558	25.47954	1858	101.4662	35.03642	1908	121.5579	45.37808	1928
104.3967	23.01336	1858	118.1974	39.63751	1908	121.3026	43.59696	1928

103.2861	23.408	1859	114.6956	23.73921	1909	120.0853	43.87708	1928
103.0361	25.33936	1859	116.1655	24.65946	1909	108.7223	39.83998	1928
103.7632	24.53009	1859	118.3212	27.04216	1910	107.9787	39.09115	1928
103.147	24.91536	1859	126.0205	44.98405	1910	109.2887	37.96067	1928
100.2477	38.17411	1860	123.9955	45.37835	1910	108.1757	36.92294	1928
103.2635	24.7619	1860	123.98	44.27301	1910	110.4936	38.82089	1928
99.16264	25.11649	1861	123.5019	43.51051	1910	110.6322	19.66999	1928
103.5768	25.42875	1861	124.6373	44.03825	1910	124.2847	45.50091	1929
102.7978	24.89611	1862	124.2157	43.39086	1910	123.0774	44.80679	1929
102.6263	25.03859	1862	125.1732	44.42978	1910	114.8813	40.8111	1929
103.714	27.33947	1863	126.3643	45.08359	1910	119.057	27.62285	1929
103.6852	22.98654	1864	125.3169	43.88429	1910	103.3176	35.94114	1930
102.0029	23.59709	1864	126.5599	43.84874	1910	106.2377	35.75707	1930
103.8219	25.60641	1864	125.7048	44.53314	1910	106.195	37.98229	1930
103.2427	23.72339	1866	125.665	43.52231	1910	110.1803	37.75674	1930
109.1076	21.47799	1867	125.2969	43.34258	1910	110.028	37.6126	1930
99.60508	24.83007	1867	126.9423	44.40624	1910	110.2561	37.5009	1930
102.7533	24.2928	1868	128.2264	43.36457	1910	109.6615	37.13532	1930
101.9873	24.07367	1868	127.337	43.72321	1910	109.7499	38.29196	1930
98.69111	24.58979	1869	125.1451	42.91602	1910	109.3576	37.00623	1930
102.9276	24.19639	1869	125.8522	42.65106	1910	105.0486	35.69276	1931
98.49455	25.02799	1870	125.525	42.67313	1910	107.2991	36.57412	1931
98.29509	24.8097	1870	95.42882	32.36883	1910	104.4784	35.21106	1931
97.93194	24.70901	1870	119.7472	49.21623	1910	122.028	45.09037	1931
99.84448	25.24785	1870	108.8422	38.59475	1910	106.6914	38.81072	1931
97.95829	24.36097	1870	105.9088	36.9788	1910	111.0763	39.01783	1931
102.162	24.67245	1870	126.6548	45.74381	1910	110.1191	37.08587	1931
108.6174	21.95302	1871	123.9624	47.33968	1910	110.7334	37.4534	1931
104.1008	26.22309	1871	126.5975	45.9869	1910	120.0022	26.89097	1932
110.2481	21.37809	1872	127.4793	45.75172	1910	104.6249	35.58231	1932
100.1291	24.44748	1873	126.9825	45.55022	1910	124.0193	45.00539	1932
99.5225	25.46365	1874	123.4136	41.80175	1911	119.8974	42.28544	1932
100.0902	23.88161	1874	123.8426	42.2994	1911	111.071	39.02925	1932
104.3339	23.60973	1874	121.231	41.53128	1911	122.8855	45.31111	1933
104.1932	24.04491	1874	122.822	41.99316	1911	100.9924	36.89983	1934
110.9438	22.35751	1875	123.7591	42.61517	1911	119.6353	27.97413	1935
103.5452	27.19398	1875	122.1091	41.68959	1911	75.19174	39.7019	1935
110.2801	21.60949	1877	124.1134	42.77858	1911	102.0317	35.93999	1936
102.4206	23.371	1877	120.3329	40.32872	1911	108.4821	22.7556	1936
105.0627	24.04994	1878	123.4074	42.50441	1911	108.897	24.78294	1936
110.3543	21.27462	1879	125.0307	41.72803	1911	107.0634	22.13656	1936
105.6168	23.6267	1879	123.346	42.74342	1911	108.5897	23.43641	1936
99.98602	35.59005	1880	120.8442	40.75547	1911	110.2947	25.24439	1936
109.1884	21.67143	1880	120.7064	40.61904	1911	107.3488	22.4071	1936

113.7465	23.0442	1880	122.7439	41.5303	1911	108.056	24.6989	1936
103.9884	24.83249	1880	124.7146	42.73689	1911	107.1357	23.08134	1936
109.9726	20.90187	1882	123.4236	41.15719	1911	110.1472	22.62443	1936
112.783	22.25317	1882	122.5307	42.38269	1911	107.3709	24.51369	1936
109.5689	19.51414	1882	123.7907	41.84797	1911	106.2277	24.29708	1936
104.302	24.88374	1882	124.1191	41.30099	1911	106.4172	23.13285	1936
118.0831	24.46422	1884	124.0363	42.53833	1911	111.2377	23.42345	1936
117.8488	24.41321	1884	121.1289	41.1187	1911	101.2645	36.68704	1937
113.031	22.52559	1885	122.0927	41.16343	1911	108.665	24.06742	1937
118.1466	24.73455	1886	124.0662	40.45892	1911	111.5414	24.41642	1937
100.4479	21.95937	1886	121.6104	38.91778	1911	109.2673	22.68543	1937
102.5641	23.88854	1886	121.7086	39.10674	1911	109.678	23.96033	1937
117.8139	24.45104	1887	121.2619	38.81638	1911	101.6176	37.37544	1938
117.6542	24.51591	1887	116.3684	39.92474	1911	109.5983	25.78434	1938
115.079	41.99178	1887	117.191	39.13837	1911	109.4563	22.91802	1938
107.4022	37.78421	1887	119.7453	40.0052	1911	111.1533	25.49074	1938
118.3796	24.96221	1888	119.4184	39.86105	1911	112.179	23.91822	1938
118.7917	25.03269	1888	126.9861	46.63698	1911	108.2547	24.83386	1938
119.0113	25.43737	1888	126.9609	47.45991	1911	97.84235	24.0174	1938
117.3622	24.51267	1888	126.2915	46.25736	1911	117.8442	25.69483	1939
117.4109	25.29244	1888	127.3975	46.07614	1911	109.7344	24.488	1939
116.188	40.95657	1888	128.0328	45.94728	1911	108.6915	24.78003	1939
110.3392	20.04342	1888	128.7426	45.97459	1911	110.5498	22.85951	1939
110.3444	19.99873	1888	127.5042	46.87581	1911	108.0948	23.93382	1939
118.576	24.81826	1889	126.1031	46.68204	1911	110.6403	26.03798	1939
118.6886	25.36392	1889	125.2689	45.70455	1911	110.9199	23.38125	1939
119.2949	26.07228	1890	125.3222	46.40182	1911	109.2325	23.73372	1939
117.6087	24.1167	1890	129.4624	44.34441	1911	106.7536	22.1108	1939
110.8485	21.92401	1890	126.2971	45.37418	1911	109.9829	24.98882	1939
110.772	21.43713	1890	129.5585	46.3177	1911	114.2798	23.16398	1939
111.9525	21.84948	1890	128.8285	45.83607	1911	119.1226	28.07446	1940
113.5826	23.5524	1890	127.1512	44.91756	1911	121.549	29.87387	1940
118.2907	25.32623	1891	128.3274	45.45656	1911	119.0491	28.99305	1940
118.2395	25.49425	1891	130.5858	46.24953	1911	117.3598	25.97769	1941
110.6373	21.65825	1891	115.8955	24.57755	1912	117.487	27.34465	1941
110.9991	21.50853	1891	79.92814	37.11304	1912	117.3278	27.54378	1941
112.3024	22.18526	1891	81.66961	36.85157	1912	124.3759	43.16091	1941
113.1346	23.03373	1891	80.18471	37.07288	1912	107.4109	40.75593	1941
113.2473	22.83974	1891	101.6131	34.73533	1914	107.1381	40.88686	1941
102.7113	25.04284	1891	112.4512	23.02906	1914	120.0692	29.3099	1941
119.2463	25.71251	1892	119.5222	26.66602	1916	120.2271	29.26569	1941
100.6189	36.28299	1892	103.3508	34.68823	1916	117.171	26.89875	1942
117.4476	49.58275	1893	115.2539	24.10094	1916	117.9186	28.43551	1942
118.1819	25.05876	1894	114.2486	23.7333	1916	118.1851	28.43812	1942

117.7539	24.626	1894	103.5053	34.59016	1917	112.6514	42.74383	1942
113.1117	23.03223	1894	113.6414	43.85218	1917	119.5675	28.11543	1942
113.3672	22.5224	1894	114.9948	42.30691	1917	119.9086	28.4505	1942
114.1729	22.27821	1894	111.1255	40.71587	1917	117.4659	26.73206	1943
113.2542	23.13189	1894	110.0551	41.02845	1917	119.4794	28.45438	1943
113.8309	23.29204	1894	111.4516	41.09108	1917	120.2825	28.14403	1943
116.6791	23.35996	1894	112.5629	40.90499	1917	120.651	28.01619	1943
116.998	23.67447	1894	111.825	40.37921	1917	120.9592	28.12304	1943
116.6908	24.35502	1894	111.6758	39.90902	1917	116.6354	27.55701	1944
116.0569	24.2759	1894	112.4884	40.52815	1917	116.5302	27.21242	1944
115.7207	24.14595	1894	113.1562	40.43969	1917	120.6896	28.15483	1944
110.3188	19.7003	1894	110.2382	40.43127	1917	120.0622	28.6494	1944
77.25114	38.41705	1894	112.6259	41.27242	1917	120.6266	27.78376	1944
118.586	24.91405	1895	111.694	41.5228	1917	118.1814	26.17253	1945
117.5338	25.00353	1895	113.1787	41.45253	1917	116.9135	27.29218	1945
119.7785	25.51008	1895	113.8884	40.87956	1917	122.8359	45.61636	1945
113.547	22.20083	1895	108.2664	41.09967	1917	100.578	35.25422	1945
114.4662	22.80053	1895	108.071	41.29025	1917	121.7357	45.8442	1945
119.1338	26.15047	1896	107.0014	40.32598	1917	122.9015	46.72482	1945
117.785	26.39796	1896	110.0301	40.40508	1917	123.4122	46.39288	1945
120.3065	23.30782	1896	111.6681	40.81791	1917	121.6129	42.38239	1946
120.2848	22.63968	1896	109.841	40.66337	1917	116.0516	27.76226	1946
121.7379	25.12991	1896	114.5676	38.14247	1917	116.3076	28.10903	1946
120.5344	23.70934	1896	115.1757	23.64252	1917	116.7763	27.90977	1946
121.4481	25.00801	1896	99.6109	22.63912	1917	116.3201	26.83947	1946
116.1691	23.29881	1896	124.8125	45.12075	1918	119.1453	42.35039	1946
116.2878	23.03703	1896	122.2606	43.61292	1918	105.7247	35.96603	1946
115.3336	22.9717	1896	109.9969	39.81297	1918	120.0866	27.79087	1946
121.608	25.0028	1897	113.8365	38.37437	1918	119.5559	42.19606	1947
121.3045	24.99259	1897	118.0437	40.42176	1918	115.9056	28.65572	1947
120.9727	24.80178	1897	114.1623	40.11345	1918	120.9016	44.5549	1947
120.5379	24.08286	1897	111.1334	39.38051	1918	118.6998	41.92563	1947
120.4265	24.05712	1897	112.1901	39.08651	1918	119.0212	42.93254	1947
111.5623	22.77085	1897	113.6869	39.69662	1918	118.51	44.19179	1947
116.5967	23.26249	1897	112.2825	39.52148	1918	119.4651	29.21736	1947
117.3028	24.36237	1898	112.2948	38.99878	1918	120.2095	27.33341	1948
100.2418	34.4737	1898	114.2744	39.76079	1918	117.0736	28.69918	1948
120.6736	24.15135	1898	112.703	39.99866	1918	119.675	43.79515	1948
120.4427	23.48035	1898	112.7327	38.4084	1918	119.2567	44.04846	1948
116.683	23.4524	1898	113.2668	39.18889	1918	119.1721	29.03191	1948
115.641	22.94379	1898	112.6927	36.75614	1918	100.1356	37.32567	1949
116.7264	24.72672	1899	113.183	39.56194	1918	114.608	41.85154	1949
118.9325	25.87073	1899	113.2875	40.09259	1918	94.35586	38.80346	1950
118.1718	26.64164	1899	113.0977	39.82666	1918	82.88461	44.60607	1952

122.4027	40.65688	1899	114.0837	40.41827	1918	95.29822	32.89511	1953
122.3578	40.40146	1899	111.5661	38.70155	1918	98.09125	36.30063	1953
120.6771	23.91138	1899	113.7485	40.36246	1918	97.00934	33.00621	1954
120.2607	23.32323	1899	112.9435	39.06382	1918	94.30637	39.62597	1956
121.5463	23.75213	1899	112.952	38.48679	1918	99.0213	37.29977	1956
120.4809	22.67709	1899	112.8568	36.83556	1918	101.087	38.77985	1957
119.568	23.56571	1899	112.8267	39.51696	1918	115.9993	42.25186	1957
113.0836	22.5797	1899	112.4227	39.3154	1918	99.89941	33.9698	1958
116.764	23.46532	1899	111.8335	38.90896	1918	100.7562	38.38463	1963
						95.61265	33.85423	1964

481